Energy surfaces and electronic properties of hydrogen fluoride

Michael Springborg
Nordisk Institut for Teoretisk Atomfysik (NORDITA), Blegdamsvej 17, DK-2100 København Ø, Denmark
(Received 19 January 1988)

Results of first-principles calculations on a single hydrogen fluoride molecule as well as on polymeric hydrogen fluoride are reported. The results are compared with other theoretical calculations as well as with experiments and the agreement is found to be good. A model for solitonic excitations is proposed and examined. The parameters entering the model are extracted from the first-principles calculations. The model represents the first attempt to include electronic interactions in the discussion of solitonic excitations in hydrogen-bonded polymers. It predicts the soliton to be a sharp kink and that the soliton induces electronic states slightly outside the energy bands of the unperturbed system. The first-principles results are also used in investigating the frozen optical stretch phonons at the zone center within both a harmonic and an anharmonic approximation. The latter is found to give rise to an extra mode compared with the former. Finally, we compare our total energies with those predicted by various proposed model potentials for describing dynamical properties of the gas and liquid phases. Some discrepancies are found, and it is argued that variations in the molecular bond length as well as electronic interactions are to be included in realistic model potentials.

I. INTRODUCTION

Hydrogen fluoride crystalizes in an orthorhombic structure[1] consisting of parallel chains of polymeric hydrogen fluoride with a smallest interchain distance equal to 6.05 a.u. Each chain has a planar zigzag arrangement of the fluorine atoms (see Fig. 1) with the hydrogen atoms placed asymmetric between neighboring fluorine atoms. X-ray diffraction has shown that the F—F nearest neighbor distance, d_F, is 4.71 a.u.,[1] the F—F—F bond angle, α, is 120.1°,[1] and from NMR spectroscopy the smallest hydrogen fluorine distance, d_H, is found to be 1.80 a.u. (Ref. 2).

The cohesion of hydrogen fluoride can be interpreted as being due to weak van der Waals and dipolar interactions between the chains, whereas hydrogen bonds between diatomic HF monomers are responsible for the intrachain cohesion. Because of its structural simplicity and of the small energies related to the interchain and intermonomer interactions, hydrogen fluoride may serve as a prototype of the very big class of compounds with bonds that are so weak that they can play a part in reactions at room temperature.

Most of the properties of hydrogen fluoride can be ascribed to isolated chains thereby neglecting the interchain interactions. Furthermore, properties of a single chain may also be relevant for studying gaseous and liquid hydrogen fluoride. Infrared (ir) measurements on gaseous HF have shown that under normal conditions the molecules are primarily found as cyclic hexamers,[3] and ir experiments on the liquid suggest that this phase consists of zigzag chains which in contrast to the solid need not be planar.[4,5] In all three phases the HF monomers tend to cluster such that they have the same local

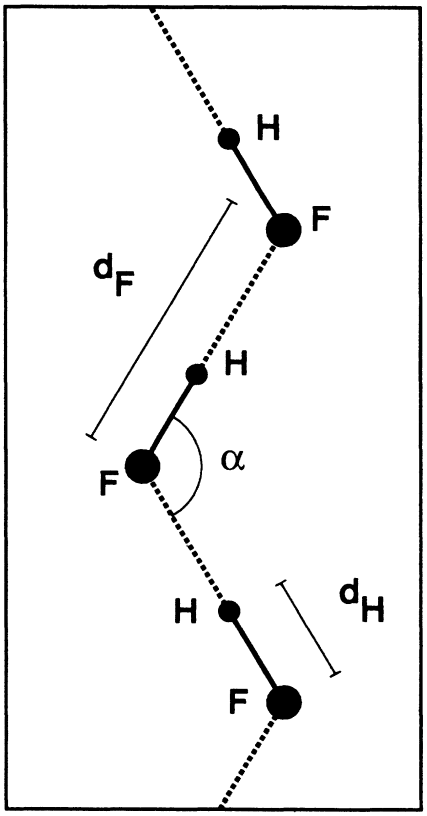

FIG. 1. The geometry of a single hydrogen fluoride chain. The solid (dashed) lines represent the molecular (hydrogen) bonds. We will refer to structures with $\alpha = 120°$ (180°) as zigzag (linear) structures.

surroundings.

In this paper we present results derived from self-consistent, first-principles calculations on a single hydrogen fluoride chain. We have calculated the electronic ground state properties for a large number of fixed values of the geometrical parameters α, d_F, and d_H. The method is described in detail elsewhere[6] but a small introduction is given in Sec. II. In Sec. III we report results of calculations on a single HF monomer. Section IV contains self-consistently obtained total energies, single-particle energies, and electron densities for the polymer. A preliminary account of parts of these results has been given earlier[7] but here we focus on using them in predicting properties of solitonic excitations (Sec. V), calculating phonon frequencies (Sec. VI), and in examining model potentials for describing dynamical properties of gaseous and liquid hydrogen fluoride (Sec. VII). Finally, we conclude in Sec. VIII.

II. THE FIRST-PRINCIPLES METHOD

For fixed positions of the nuclei (the Born-Oppenheimer approximation) we seek the single-particle eigenvalues, ε_j, and eigenfunctions, $\psi_j(\mathbf{r})$ to the Kohn-Sham equations[8] in Rydberg atomic units

$$\hat{H}\,\psi_j(\mathbf{r})=[-\nabla^2+V(\mathbf{r})]\,\psi_j(\mathbf{r})=\varepsilon_j\psi_j(\mathbf{r}), \tag{1}$$

where the potential $V(\mathbf{r})$ is the sum of the Coulombic potential of the nuclei, $V_N(\mathbf{r})$, that of the electrons, $V_e(\mathbf{r})$, and the exchange-correlation potential, $V_{xc}(\mathbf{r})$. For the latter we use the Barth-Hedin local approximation[9] such that it becomes a simple function of the electron density:

$$V_{xc}(\mathbf{r})=V_{xc}[\rho(\mathbf{r})], \tag{2}$$

with

$$\rho(\mathbf{r})=\sum_j |\psi_j(\mathbf{r})|^2, \tag{3}$$

where the sum goes over all occupied levels.

The potential can be expanded around each nucleus in angular dependencies:

$$V(\mathbf{r})=\sum_L V_L(r_R)\,Y_L(\hat{r}_R), \tag{4}$$

where $\mathbf{r}_R=\mathbf{r}-\mathbf{R}$, and the nucleus is assumed placed at $\mathbf{R}$.

The eigenfunctions, $\psi_j(\mathbf{r})$, are expanded in linearized muffin-tin orbitals (LMTO's). They are defined as being numerical solutions of (1) with the potential being replaced with the spherical component [i.e., $L=(0,0)$] of (4) inside nonoverlapping muffin-tin spheres centered on the nuclei. On the spheres they are matched smoothly to spherical Hankel functions, $h_l^{(1)}(\kappa r_R)Y_L(\hat{r}_R)$, $\kappa^2<0$. The basis functions are hence defined as being eigenfunctions of a muffin-tin potential but in setting up the Hamiltonian matrix the *full* potential is considered. This is done by including the full expansion (4) inside the muffin-tin spheres and by fitting the potential in the interstitial region outside all muffin-tin spheres to a sum of overlapping, atom-centered spherical Hankel functions. For details, see Ref. 6.

For the polymer of Fig. 1 the "helical" (translational or zigzag) symmetry is explicitly taken into account by defining basis functions in local atom-centered right-handed coordinate systems with the z axis parallel to the polymer axis and the x axis pointing away from it. Bloch waves are formed from the local basis functions. Accordingly, the unit cell of polymeric hydrogen fluoride contains only a single HF monomer for all values of α.

The sizes of the muffin-tin spheres were kept constant for all calculations. s, p, and d functions were included on both fluorine and hydrogen atoms, and the basis set was doubled by having two fixed, common κ values for both atoms and all l's. However, due to almost linear dependencies, those linear combinations of the basis functions that corresponded to the smallest eigenvalues of the overlap matrix were excluded.[10] The size of the basis set was therefore 32 functions per monomer.

Since polymeric hydrogen fluoride is expected to be an insulator with narrow energy bands we use only six k points in half part of the Brillouin zone.

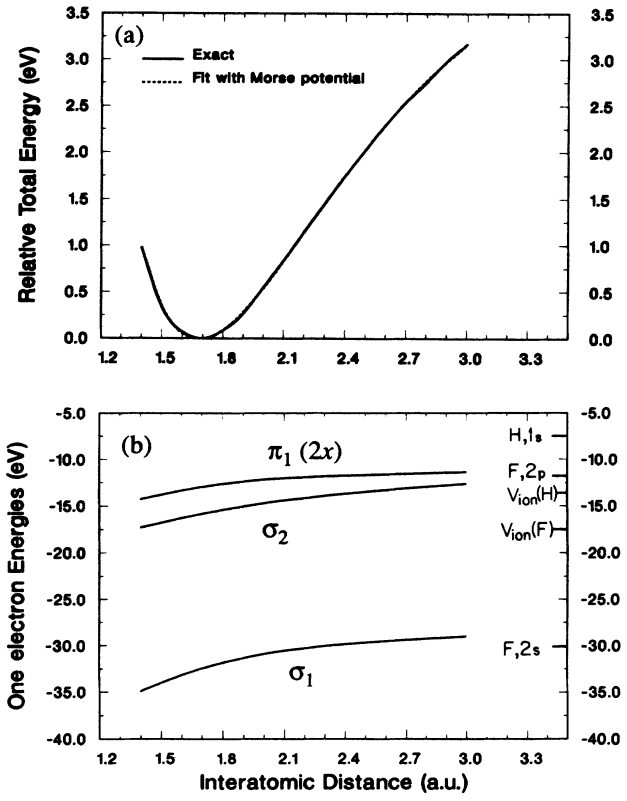

FIG. 2. (a) Total energy of a single HF monomer as a function of the bond length. The curve labeled "exact" is the results of the first-principles calculations, the other the result of the fit of the exact curve with a Morse potential. Note, that the two curves are very close to each other. (b) The single-particle valence energies of the monomer as a function of bond length. The four orbitals split into two single degenerate σ orbitals and one double degenerate π orbital. To the right the local (spin) density single-particle valence energies of the isolated atoms as well as their experimentally found first ionization potentials (IP) are shown.

III. THE HF MONOMER

First we consider a single monomer, i.e., the limit $d_F \to \infty$. In Fig. 2 we depict the total energy [Fig. 2(a)] and the single-particle eigenvalues ε_j [Fig. 2(b)] as a function of the molecular bond length d_H.

The minimum for the total energy is found for $d_H = 1.70$ a.u. in good agreement with the experimental values 1.71 a.u. (Ref. 11) and 1.73 a.u. (Ref. 12). *Ab initio* Hartree-Fock calculations[13] give $d_H = 1.70$ a.u.

As shown in Fig. 2(a) we can fit the total energy in the range 1.4–3.0 a.u. very well with a Morse potential

$$E_M = D_0\{1-\exp[-\beta_0(r-r_0)]\}^2 \tag{5}$$

except for an additive constant. The parameters are $D_0 = 4.63$ eV, $\beta_0 = 1.334$ a.u., and $r_0 = 1.684$ a.u., and the root-mean-square deviation (rmsd) was found to be only 0.009 eV showing how good the fit is in this range. The minimum of the Morse potential is slightly shifted away from the position of that of the total energy. As a very careful inspection of Fig. 2(a) shows the Morse potential fit tends to underestimate the total-energy for d_H close to 3.0 a.u. The dissociation energy predicted by the Morse potential fit (D_0) is therefore smaller than the experimental value [6.12 eV (Ref. 11)]. On the other hand, the properties close to the equilibrium are excellently described by the fit. Using (5) in describing the total energy of the molecule the vibrational eigenvalue spectrum becomes[14]

$$e_n = (n+\tfrac{1}{2})\omega_e hc - (n+\tfrac{1}{2})^2\omega_e x_e hc, \tag{6}$$

with

$$\omega_e hc = \hbar\beta_0(2D_0/\mu)^{1/2}, \qquad x_e = (\omega_e hc)/(4D_0). \tag{7}$$

Here, μ is the reduced mass. The vibrational frequencies are then

$$\nu_n = e_n - e_0 = n\omega_e hc - n(n+1)\omega_e hc x_e, \tag{8}$$

which is $[4089n - 112n(n+1)]$ cm^{-1} for HF and $[2964n - 59n(n+1)]$ cm^{-1} for DF. For HF the first five calculated vibration frequencies (with the experimental values of Di Lonardo and Douglas[11] in parentheses) are (in cm^{-1}) 3865 (3961), 7506 (7750), 11 034 (11 372), 14 118 (14 831), and 17 088 (18 130). We see that the agreement is good for the lowest frequencies but that it becomes worse for the higher ones due to the wrong description of the dissociation. The anharmonicity [last term in Eq. (8)] is found to be important; without it the fifth frequency would have been 20 445 cm^{-1}. *Ab initio* Hartree-Fock calculations on the HF monomer[13] yield 4272 and 8383 cm^{-1} for the first two vibrational frequencies, whereas inclusion of correlation gives[15] 3593 and 7728 cm^{-1}, respectively.

For DF we find the first two frequencies to be 2847 and 5576 cm^{-1}.

Although the single-particle energies calculated within the density functional formalism in principle are not to be related with excitation energies experience has shown that it is a good approximation to neglect this formality. In Fig. 2(b) the valence energies for the HF monomer are shown as a function of d_H. Furthermore, the exact numerical local (spin) density quasiparticle energies for the free atoms together with their experimental ionization potentials are shown. As has been discussed by, e.g., Trickey,[16] we notice a general failure of the local (spin) density to reproduce the correct ionization potentials for the hydrogen and fluorine atoms.

In Fig. 3 we depict the electron densities for the three valence orbitals for the optimized equilibrium geometry. From Figs. 2(b) and 3 we easily realize that all valence orbitals are bonding orbitals. The uppermost valence orbital is a double degenerate π orbital formed by p orbitals perpendicular to the molecular axis, whereas the other two orbitals are of σ symmetry and formed by s and p orbitals, respectively. It is seen in Fig. 3 that the orbitals have only small hydrogen components.

The ionization potential is found to be 13.0 eV, which is considerably smaller than the experimental value[17] 16.2 eV, the *ab initio* Hartree-Fock value[18] 17.7 eV, and the *ab initio* Hartree-Fock plus correlation value[19] 16.0 eV. The error is almost the same as found for the free atoms [see Fig. 2(b) and Ref. 16], so we will ascribe it a general failure in the density functional formalism in its local approximation.

From the coefficients q_F and q_H ($q_F = -q_H$) to the long-range $1/r$ Coulomb potential centered on the nuclei we can estimate a dipolar moment of 1.62 D, which is smaller than the experimental value[12] 1.80 D. At the *ab initio* Hartree-Fock level the dipolar moment is overestimated,[13,15] being about 1.93 D, whereas inclusion of correlation reduces the error to a few percent.[15]

In closing this section we would like to point out that the calculations give results in good agreement with experiments. This is important, since we will apply *exactly* the same approximations (except, of course, for approximations in connection with summations in direct and reciprocal space) for the infinite polymer. Here, most previous parameter-free calculations (see the following section) have been performed with the Hartree-Fock method with less converged basis sets than those with which we have compared our results on the monomer.

IV. ELECTRONIC GROUND STATES OF THE HF POLYMER

We now pass to the infinite periodic polymer. In this section we will report the results of the first-principles calculations of the electronic ground state properties for various values of α, d_F, and d_H. Since the calculations have been performed with the same approximations as used for the monomer a direct comparison is possible. In three subsections we describe the calculated total energies, band structures, and electron densities, respectively.

A. Total energies

For α kept fixed we depict in Fig. 4 the relative total energy as a function of d_F and d_H. α is chosen to be 120° [Fig. 4(a)] and 180° [Fig. 4(b)]. The results have been de-

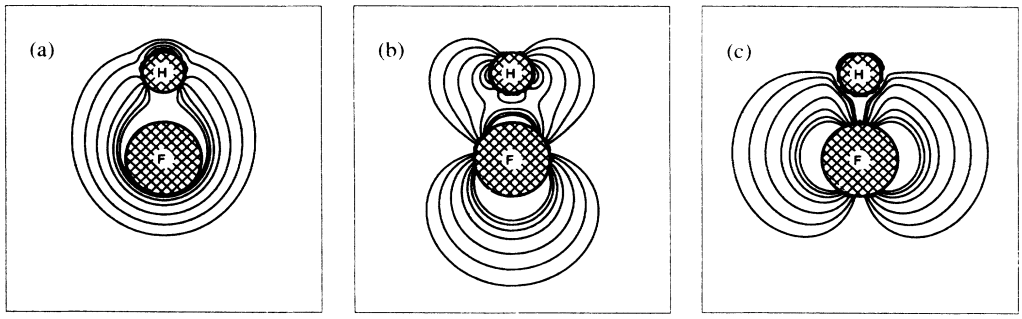

FIG. 3. The electron density outside the interior of the muffin-tin spheres for the optimized geometry of a single HF monomer for the three valence orbitals, (a) the σ_1 orbital, (b) the σ_2 orbital, and (c) the π_1 orbital. The contour values are 0.10, 0.08, 0.06, 0.04, 0.02, 0.01, and 0.005 a.u.

scribed in detail in our earlier report[7] so we will here mainly give a short discussion of them, sufficient for understanding the following sections. Furthermore, we will make a detailed comparison with earlier works on polymeric hydrogen fluoride. This is done in order to make an evaluation of the results of this work and of others presented in the following sections possible.

Interchanging the molecular and hydrogen bonds in the structure of Fig. 1 gives a structure with the same total energy. This symmetry manifests itself in a symmetry of the total energy about the point $d_H = d_F/2$ for fixed α and d_F as seen in Fig. 4.

For $\alpha = 120°$ we find a minimum for $(d_F, d_H) = (4.77, 1.87)$ a.u. The energy related to the hydrogen bond (hereafter denoted E_H and defined as the total energy of the isolated optimized monomer minus that per monomer of the polymer) is found to be 0.61 eV. For α kept fixed at 120° the smallest barrier for a collective shift of *all* the protons to the energetically equivalent position (i.e., $d_H \rightarrow d_F - d_H$) is found for $d_H = d_F/2 = 2.28$ a.u., where the barrier height is 0.30 eV.

For $\alpha = 180°$ we find indications of two local minima [see Fig 4(a)]. However, the energy barrier between them is so small (0.05 eV) that we cannot exclude it being a numerical artifact. The two minima are found for $(d_F, d_H) = (4.39, 1.94)$ a.u. and $(4.80, 1.89)$ a.u., respectively. The hydrogen bond energy (E_H) for these is the same (0.31 eV) within 0.01 eV for the two structures. Since the length of the unit cell is $d_F \sin(\alpha/2)$ the zigzag structures are more compact than the linear structures for the same value of d_F. Therefore, in the range of d_F (i.e., $d_F \sim 4-5$ a.u.) where not only nearest neighbor interactions but also next-nearest neighbor interactions (e.g., dipole and quadrupole interactions) are important, the total energy of the more open linear structures will show a weaker dependence on d_F than the zigzag structures will. Hence, the area circumscribed by the innermost contour curve in Fig. 4(b) is larger than that of Fig. 4(a). Therefore, the energy barrier for a collective shift of all the protons from one minimum to the symmetry equivalent minimum is smaller for the linear than for the zigzag structures. The smallest barrier height is for $\alpha = 180°$ found to be 0.18 eV for $d_H = d_F/2 = 2.16$ a.u.

Varying all three parameters α, d_F, and d_H but still restricting ourselves to polymers of the type sketched in Fig. 1 we find a global minimum for $\alpha = 125°$, $d_F = 4.72$

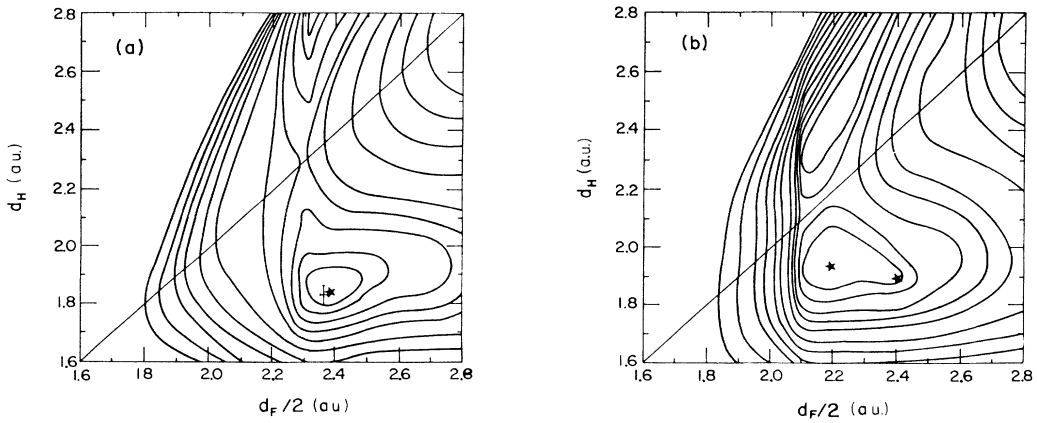

FIG. 4. Relative binding energy per HF monomer for the polymer of Fig. 1. The energy is plotted as a function of $d_F/2$ and d_H for α kept constant at 120° (a) and 180° (b). The local minimum in (a) corresponds to a hydrogen bond energy of 0.61 eV; those of (b) to 0.31 eV. Contour values are 2.0, 1.5, 1.25, 1.0, 0.75, 0.5, 0.4, 0.3, 0.2, 0.1, and 0.05 eV relative to the local minima of each figure.

a.u., and $d_H = 1.85$ a.u. The hydrogen bond energy, E_H, of this structure is 0.64 eV. The geometry is to be compared with the experimental values[1,2] quoted in the beginning of this paper, i.e., $\alpha = 120.1°$, $d_F = 4.71$ a.u., and $d_H = 1.80$ a.u., or with the more recent work[20] on deuterium fluoride, i.e., $\alpha = 116°$, $d_F = 4.72$ a.u., and $d_H = 1.83$ a.u. We find the agreement to be good. Since the hydrogen bond energy of a HF dimer is 0.30 eV[12] and since that of the polymer is expected to be roughly 50–100 % larger[21] our value of E_H seems to be reasonable.

Comparing Figs. 2(a) and 4 we see that for fixed d_F the optimal value of d_H for the polymer only slowly approaches the optimized value of the monomer as a function of increasing d_F.

There exist a number of papers on calculations of total energies of polymeric hydrogen fluoride or related structures. However, most of them either are based on semiempirical methods or consider a fairly limited number of geometries within the Hartree-Fock method where correlation effects per definition are excluded. We will now discuss the results of some of these papers without claiming to be complete.

Santry and co-workers[22,23] used the semiempirical complete neglect of differential overlap (CNDO) method in examining the relative stability of a monomer, a dimer, a polymer, and the two crystal structures where neighboring chains are parallel or antiparallel. They find E_H for the polymer to be 0.55 eV, in good agreement with our value.

Also Karpfen *et al.*[21] applied the CNDO method. Their hydrogen bond energy for the zigzag structure, 0.61 eV, is in excellent agreement with ours, but that of the linear structure, 0.60 eV, is significantly larger than ours. This might be due to the lack of a proper parametrization of the CNDO method for this nonexisting structure.

A very detailed analysis was undertaken by Zunger[24] within the semiempirical intermediate neglect of differential overlap (INDO) method. He considered the total energy for a large number of geometries as done in the present work. His optimized structure has $\alpha = 122°$, but surprisingly $d_H = d_F/2 = 2.13$ a.u. The hydrogen bond energy is significantly overestimated, 1.28 eV. Fixing d_F at 4.71 a.u. he finds $\alpha = 124°$, $d_H = 1.92$ a.u., and $E_H = 0.78$ eV.

Finally, Lochmann[25] has also performed semiempirical calculations on polymeric HF. His method, perturbative configuration interaction using localized orbitals for crystal calculations (PCILOCC), gave quite small hydrogen bond energies: 0.22 eV for both zigzag and linear structures.

Kertész *et al.*[26] have calculated an *ab initio* Hartree-Fock hydrogen bond energy of 0.44 eV for a fixed zigzag geometry.

Karpfen and co-workers[27–29] have within the *ab initio* Hartree-Fock approximation considered a limited number of geometries of both linear and zigzag chains. They report optimized structures with $\alpha = 129.7°$, $d_F = 4.91$ a.u., $d_H = 1.74$ a.u., and $E_H = 0.28$ eV for the zigzag polymer, and $d_F = 5.05$ a.u., $d_H = 1.72$ a.u., and $E_H = 0.26$ eV for the linear polymer. These values are in considerably worse agreement with the experimental values than ours.

I'Haya *et al.*[30] reported *ab initio* Hartree-Fock as well as model potential calculations on fixed linear and zigzag geometries. They report very varying energy differences for equivalent calculations on the two structures: from 0.21 eV to 12.2 eV. We have no explanation of this large spread, which seems very unsatisfactory.

Otto and Steinborn[31] have included parts of the correlation effects perturbatively on results from an *ab initio* Hartree-Fock calculation for a fixed geometry of the three-dimensional crystal structure. They report a hydrogen bond energy for the single chain of 0.39 eV (0.40 eV) without (with) correlation effects.

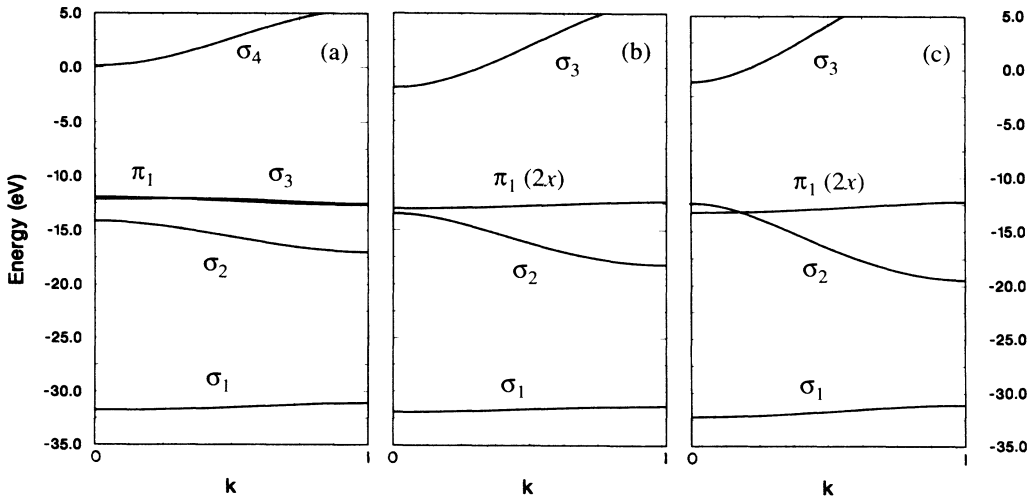

FIG. 5. The energy bands for the structures of the three local minima of Fig. 4. The bands are drawn as functions of a dimensionless k number with $k = 0$ being the zone center and $k = 1$ being the zone edge. (a) The zigzag structure, and (b) and (c) the linear structures with the large (b) and small (c) d_F value, respectively. All bands are fully occupied except the uppermost which is empty.

Finally, Jansen *et al.*[32] have presented a very detailed examination of some solid hydrogen halides. For HBr they applied the density functional formalism and the pseudopotential method on linear chains (i.e., for simplification they did not consider the experimental known structure with zigzag chains) for a number of bond lengths equivalent to Fig. 4(b). As they should, the results resemble many similarities with Fig. 4(b). To our knowledge this is the only other example of application of the density functional formalism on systems containing hydrogen bonds. For HF they used the *ab initio* Hartree-Fock method on the cyclic hexamer. Their optimized values of d_F and d_H are 4.81 and 1.70 a.u. corresponding to slightly too long (short) hydrogen (molecular) bonds as also the *ab initio* Hartree-Fock calculations by Karpfen *et al.*[27–29] gave, and their hydrogen bond energy seems to be too large, 1.58 eV. For a collective shift of all the protons to the symmetric position the smallest barrier ($\sim$0.25 eV) is found for $d_H = d_F/2 = 2.12$ a.u.

In total we find that our results show the best general agreement in structural parameters and total energies compared with the experimental values.

B. Band structures

For the three local minima of Fig. 4 we depict in Fig. 5 the single-particle eigenvalue spectra. For all three structures the valence bands are easily related to the molecular eigenvalues of Fig. 2(b). For the zigzag structure the lower symmetry splits the double degenerate molecular π_1 level up into a σ_3 and a π_1 band as seen in Fig. 5(a).

The bandwidths of the zigzag structure and of the "long" linear structure [i.e., that local minimum in Fig. 4(b) which has the larger d_F value, in contrast to the other, "short," linear structure] are quite similar: 0.7 eV (σ_1), 2.9 eV (σ_2), 0.5 eV (σ_3), and 0.7 ev (π_1) for the zigzag structure, and 0.6 eV (σ_1), 4.7 eV (σ_2), and 0.7 eV (π_1) for the long linear structure. Since the two structures have similar molecular and hydrogen bond lengths, and since the molecular orbitals are well localized close to the sin-

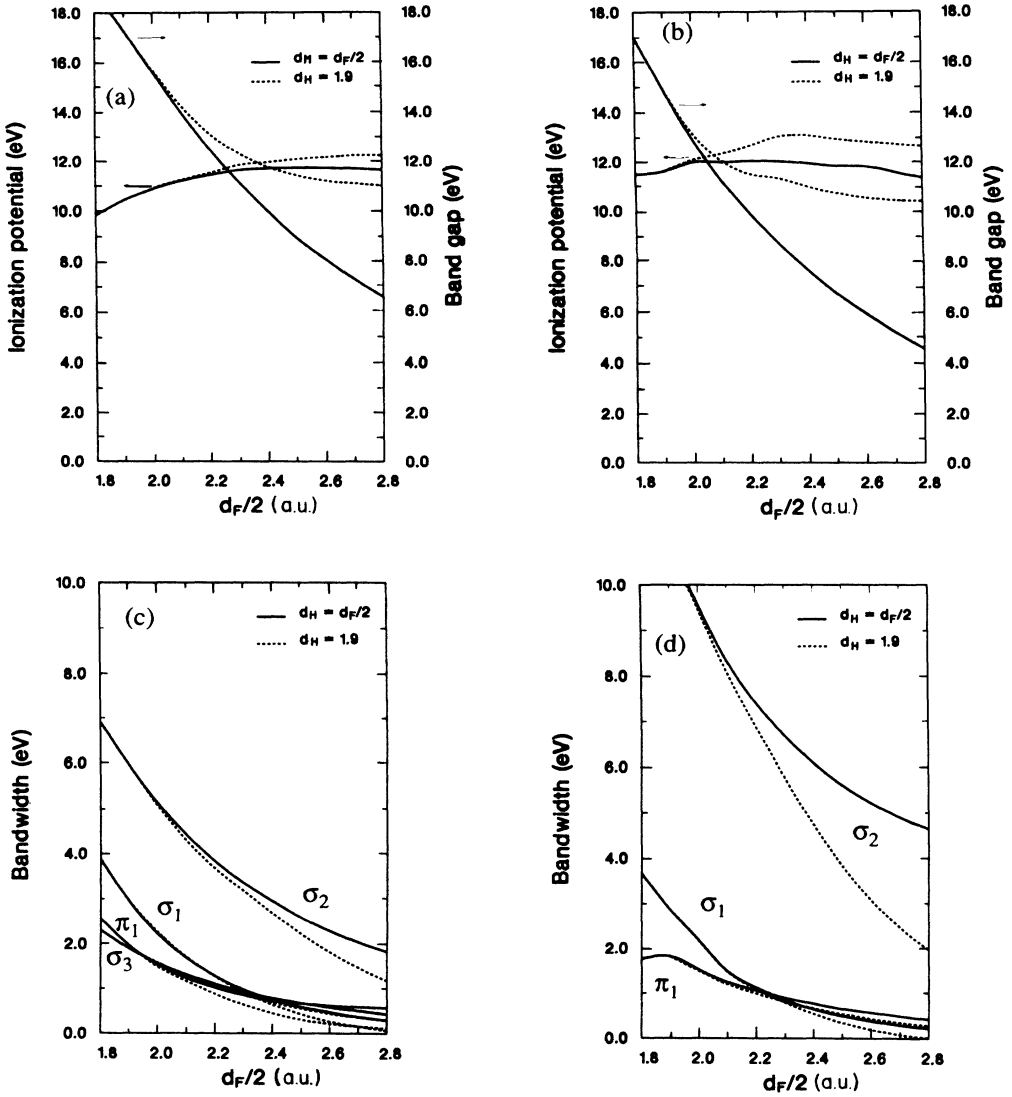

FIG. 6. Ionization potential and band gap [(a) and (b)] and valence bandwidths [(c) and (d)] for the zigzag [(a) and (c)] and linear [(b) and (d)] structures as a function of d_F for the two cases $d_H = d_F/2$ (solid curves) and $d_H = 1.9$ a.u. (dashed curves).

gle monomer (cf. Fig. 3), the bandwidths should mainly be determined from nearest neighbor interactions only. There is one difference in the bandwidths: the σ_2 band originating from the molecular σ_2 orbital of Fig. 3(b). This orbital is more delocalized and shows a specific directional elongation such that the overlap of these depends on their relative orientation leading to the quoted differences in the bandwidths.

From these considerations it can also be understood why the bandwidths of the short linear structure are somewhat larger, i.e., 1.1 eV (σ_1), 7.0 eV (σ_2), and 1.0 eV (π_1).

The ionization potential for the three structures is calculated to be 11.9, 12.3, and 12.2 eV, respectively, i.e., slightly smaller than that of the monomer. A similar decrease has been noticed by Liegener and Ladik[19] in their *ab initio* Hartree-Fock plus correlation calculations.

The band gap, which in general is substantially underestimated in local density calculations, is found to be 12.1, 10.5, and 11.1 eV for the three structures, respectively, and the compound is hence a large-gap insulator.

Our bandwidths are considerably smaller than those reported by Karpfen *et al.*[21] from their CNDO calculations. Furthermore, Karpfen *et al.* did not in general find the σ_2 band to be much wider than the other bands. Also their ionization potentials were larger than ours, but here—as discussed for the monomer—we expect the local density approximation to give too small values for HF. The total valence bandwidth, which normally is reproduced well within the local density approximation, was by Karpfen *et al.* found to be some few eV larger.

The INDO bands of Zunger[24] and the CNDO bands of Pietronero and Lipari[33] showed many similarities with those of Karpfen *et al.*[21] The larger bandwidths found by these semiempirical methods might be related to the Hartree-Fock approximation inherent in the CNDO and INDO methods. This approximation is known in general to overestimate the bandwidths.

In contrast to these results the *ab initio* Hartree-Fock calculations by Kertész *et al.*[26] and by Karpfen and co-workers[28,29] clearly gave that the σ_2 band is significantly broader than the other bands. However, unexpectedly their bandwidths were in general smaller than ours. It could be due to too small basis sets in the Hartree-Fock calculations, but their results show a decrease in the bandwidths upon increasing the basis set size. On the other hand, Liegener and Ladik[19] have demonstrated that the width of the uppermost valence band increases from 0.25 to 1.45 eV upon inclusion of correlation effects. So, the lack of correlation effects might be the reason for the too narrow bands found by Kertész *et al.*[26] and by Karpfen and co-workers.[28,29]

For the sake of completeness and for later purposes we show in Fig. 6 the ionization potential, band gap, and bandwidths for both zigzag and linear structures as a function of d_F for the high-symmetry situation ($d_H = d_F/2$) as well as for a low-energy situation ($d_H = 1.9$ a.u.). The bandwidths confirm the already es-

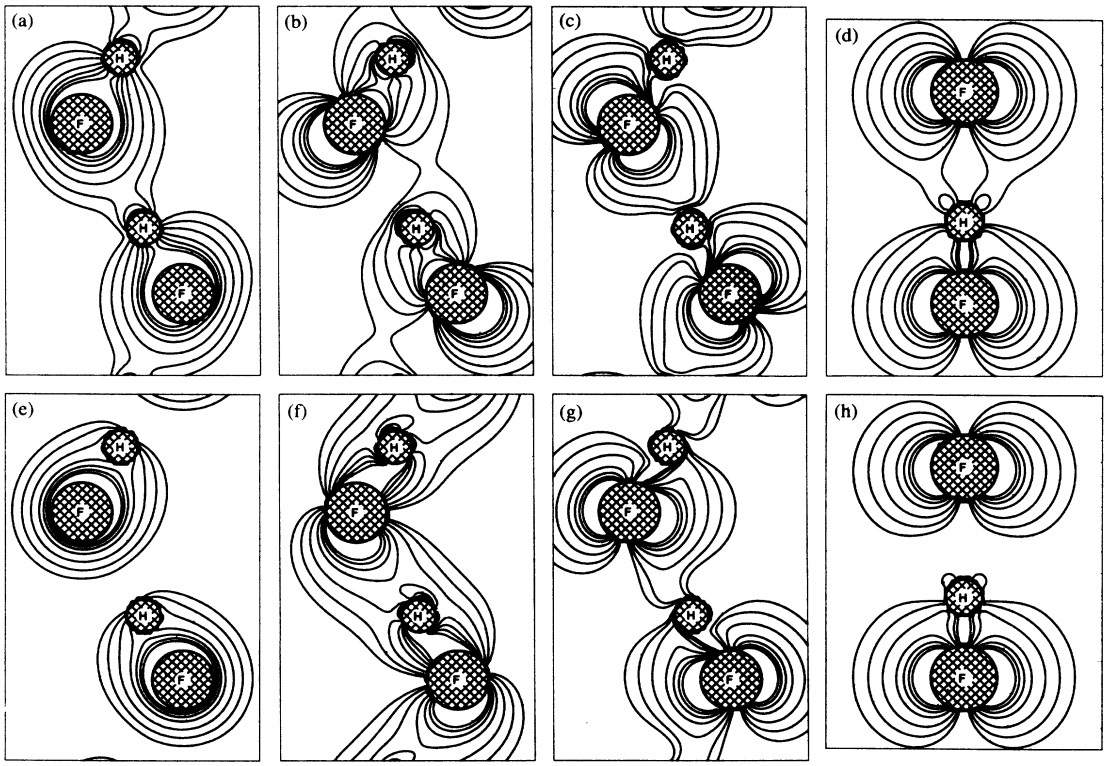

FIG. 7. Electron densities outside the interior of the muffin-tin spheres for the optimized zigzag structure for the σ_1 [(a) and (e)], σ_2 [(b) and (f)], σ_3 [(c) and (g)], and the π_1 [(d) and (h)] valence orbitals at the zone center [(a)–(d)] and zone edge [(e)–(h)]. Contour values as in Fig. 3. In (a)–(c) and (e)–(g) the plane is that of the nuclei; in (d) and (h) one perpendicular to that of the nuclei containing a proton and its two nearest fluorine neighbors.

tablished picture: they are all small except for that of σ_2, which furthermore is larger for the linear than for the zigzag structures. For $d_H = d_F/2$ the molecular orbitals become more elongated than for $d_H = 1.9$ a.u. such that the bandwidths (band gaps) become larger (smaller). As indirectly seen in Figs. 5(b) and 5(c) the nature of the top of the valence bands can shift between being of σ and being of π type. This causes the small oscillations in Fig. 6(b).

C. Electron densities

In Figs. 7 and 8 we show the electron densities of the valence orbitals at the zone center and the zone edge for the optimized zigzag structure (Fig. 7) and the optimized short linear structure (Fig. 8). Those of the long linear structure have many similarities with those shown as will be described in the following, and we have hence chosen not to include them.

The σ_1 orbitals [Figs. 7(a), 7(e), 8(a), and 8(d)] show only little interaction in the zigzag and long linear structures. Comparing Figs. 7(a) and 7(e) with Fig. 2(a) we see only a small repulsion at the zone edge [Fig. 7(e)] and accordingly only a small compression of the molecular orbitals. For the short linear structure this compression is larger.

For the σ_2 orbitals [Figs. 7(b), 7(f), 8(b), and 8(e)] we clearly see the maximal overlap when the molecular orbitals are parallel. At the zone edge it is recognized how the proton can be regarded as a "bridge" for the interaction between the elongated fluorine p orbitals; mostly for the short linear structure, less for the other two.

The molecular π orbitals, which remain degenerate in the linear structures, split into two in the zigzag structures as discussed above. One of these can interact bondingly at both zone center and zone edge [Figs. 7(c) and 7(g)] such that the top of the corresponding σ band is at a low-symmetry point in the Brillouin zone.

For the π bands the largest interaction is for the zigzag structure [Figs. 7(d) and 7(h)] whereas the interaction for the long linear structure is very small. Here, the short linear structure [Figs. 8(c) and 8(f)] is in between.

V. SOLITONIC EXCITATIONS

Many hydrogen-bonded systems have two degenerate or nondegenerate conformations, corresponding to *all* the protons of the hydrogen bonds being closer to one or the

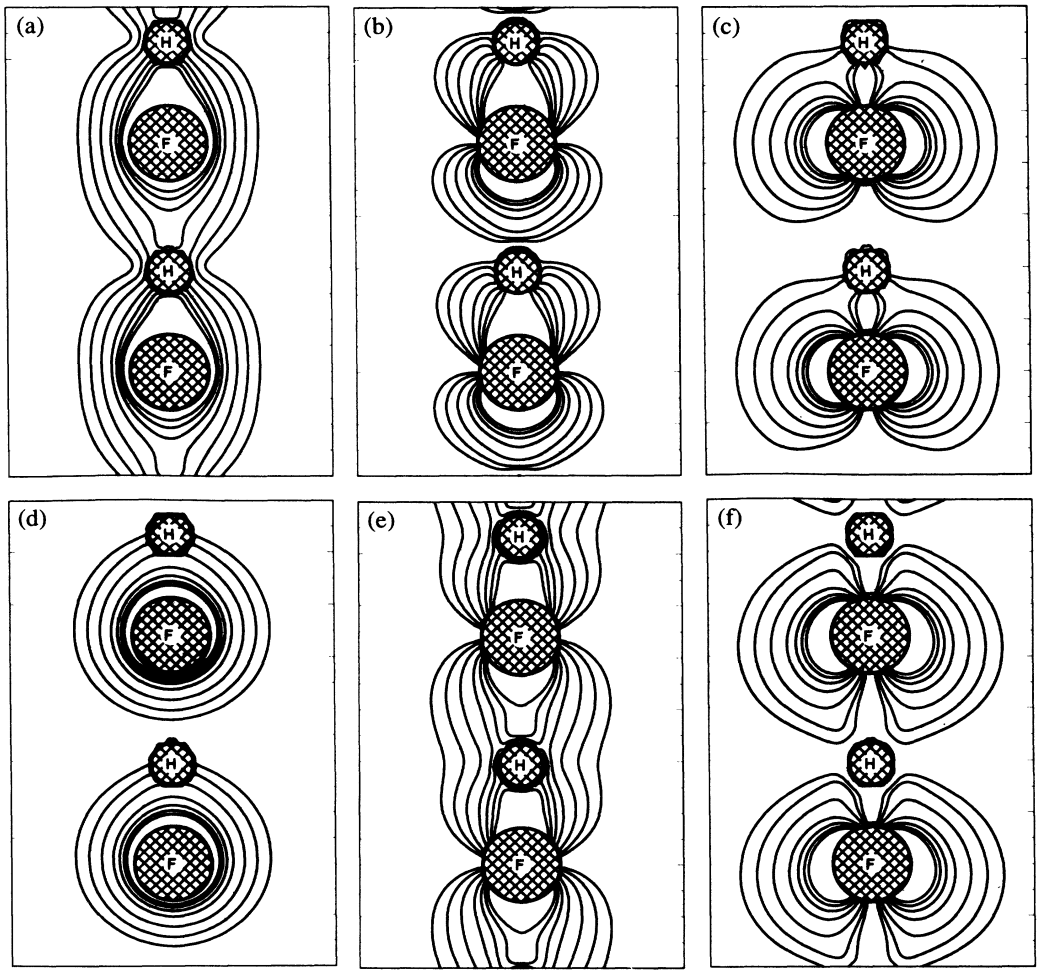

FIG. 8. As Fig. 7 but for the optimized short linear structure for the σ_1 [(a) and (d)], σ_2 [(b) and (e)], and π_1 [(c) and (f)] valence orbitals at the zone center [(a)–(c)] and zone edge [(d)–(f)].

other of their two nearest neighbors. Whether the two minima are degenerate in energy or not depends on the symmetry of the system. It has then been proposed[34] that such a system might be excited by locally creating a domain wall between two parts where in one part the protons are closer to one of their neighbors and in the other part they are closer to the other. These domain walls, the so-called solitons or kinks, can move throughout the system, and are considered important for α helices,[34-39] but they have also been considered for other systems[40] including hydrogen fluoride.[32]

Solitons are also assumed important for the excited states of the conjugated polymers of which the most well-known example is *trans*-polyacetylene. Undimerized *trans*-polyacetylene, $(CH)_x$, consists of a planar zigzag arrangement of carbon atoms each bonded to a single hydrogen atom lying in the same plane. The valence bands are filled deep lying σ bands from carbon sp^2 hybrids and hydrogen s orbitals and a half-filled π band from the last carbon p orbital. By dimerizing a gap opens up between the valence and the conduction states. Recognizing that the ground state is double degenerate corresponding to the two equivalent patterns of alternating carbon carbon single and double bonds, it has been proposed (see, e.g., Ref. 41) that domain walls (solitons, kinks) between the two patterns might be excited upon doping the polymer. The solitons induce single-particle states in the gap and these states are assumed responsible for the large conductivity observed for this compound upon doping.[42]

Since the examinations of the solitonic excitations of the hydrogen-bonded polymers most often apply a continuum version of a model Hamiltonian, and furthermore only focus on the creation energy of a soliton and not on the single-particle energies, and since the latter are important for examining the properties of the soliton excited conjugated polymers, we will here present a simple model which describes the total energy as well as the single-particle energies for both the ground state and the soliton in hydrogen fluoride. The results should then throw light on the solitons in hydrogen-bonded polymers as well as in conjugated polymers. The model is a combination of the two used for hydrogen-bonded polymers and for conjugated polymers.

We will especially focus on the consequences of two differences from polyacetylene: (i) The geometry equivalent to undimerized polyacetylene (i.e., $d_H = d_F/2$) does not have a half-filled band and the soliton induced states might therefore appear at other positions than at the middle of a gap; and (ii) the energy of formation of a soliton might be considerably larger for HF since the "dimerization" energy of HF is about one order of magnitude larger than that normally assumed for $(CH)_x$. (We will use the word "dimerization" for the process in which all the protons are shifted from the saddle point for $d_F/2 = d_H$ to one of the degenerate local minima keeping α fixed.)

In examining solitons in hydrogen fluoride we shall assume that α is constant and that the protons remain on the lines connecting neighboring fluorine atoms. Although this might not be precisely true we believe that the modifications introduced by leaving these assumptions will only be small. We shall furthermore assume that for any proton the molecular and hydrogen bond lengths $d_F - d_H$ and d_H follow a unique curve in the (d_F, d_H) plane, and that this curve for $\alpha = 120°$ corresponds to the curve connecting the two degenerate minima in Fig. 4(a). Since the bonding properties of HF mainly are determined by local interactions between neighboring molecular orbitals and slowly varying long-range electrostatic interactions (see, e.g., Ref. 7) this assumption seems justified. The curve will be a "least-descent-of-total-energy" curve and pass through the saddle point on the $d_H = d_F/2$ line. We will use a parameter x to label positions on the curve with x being the distance in the $(d_F/2, d_H)$ plane from the saddle point. $x = \pm x_{(0)}$ is the two degenerate minima. The parameters x_n are accordingly to describe the positions of the fluorine atoms with respect to those of the protons, and the model is to describe to which extent the protons participate in molecular and hydrogen bonds with the two neighboring fluorine atoms.

We will introduce a number of parameters in the model. These we will determine from the total-energy results of the perfect undistorted polymer. It should be pointed out that many of them are to be considered approximate but our results should remain almost unchanged when modifying the parameters within certain reasonable limits. Furthermore, the model is explicitly made for examining the solitonic excitations in this polymer and should therefore only with care be transferred to other properties of hydrogen fluoride. On the other hand, the model is easily modified in order to describe solitonic excitations in other hydrogen-bonded systems.

First of all, we will describe the interaction between the molecular orbitals within a tight-binding formalism. From the calculations on the monomer (Sec. III) we notice that the energies of the molecular orbital depend on the bond length. Compared with the Su-Schrieffer-Heeger model[43,44] for *trans*-polyacetylene we will therefore have additional x depending on-site matrix elements, and since we have four double occupied valence orbitals the tight-binding Hamiltonian becomes

$$E_{TB} = \sum_{s=1}^{2} \sum_{i=1}^{4} \sum_{n=1}^{N} [-t_{n,n+1}^{(i)}(x_n)(c_{n,s}^{(i)\dagger} c_{n+1,s}^{(i)} + c_{n+1,s}^{(i)\dagger} c_{n,s}^{(i)}) + \varepsilon^{(i)}(x_{n-1}, x_n, x_{n+1}) c_{n,s}^{(i)\dagger} c_{n,s}^{(i)}], \quad (9)$$

where s labels the spin variable, i the molecular orbitals, n the unit cells, and c and $c^\dagger$ are the annihilation and creation operators, respectively. In this model the hybridization between the different molecular orbitals is neglected. This is reasonable when noticing the large separation of the bands of same symmetry (cf. Fig. 5).

In a ring of N monomers (which has periodic boundary conditions) the introduction of a kink-antikink pair, each with zero width, will lead to a fluorine atom and a hydrogen atom each with no neighbors to form molecular bonds with (see Fig. 9). We will assume that in this situation the single-particle energies of the eight electrons of this hydrogen fluorine pair are determined from those of

the polymer where all the protons are placed in the symmetric position, $d_H = d_F/2$. These energies are slightly higher than those of the undistorted polymer and will therefore be reasonable estimates of the energies of the nonbonding orbitals. This model will therefore give that the soliton-antisoliton pair lead to a negatively charged fluorine ion and a positively charged hydrogen ion. We will denote the charges $\pm q$.

The soliton so created gives what has been called ionic defects[40,45] as can be understood from the discussion above and from Fig. 9(b). Another possible defect is the so-called oriental defect,[40,45] where the soliton is a domain wall between two orientations of the monomers and where there then are two identical ions as next neighbors across the kink. Neither this possibility nor the possibility that the kink-antikink pair generates a HFH triple and a single F atom will be considered here.

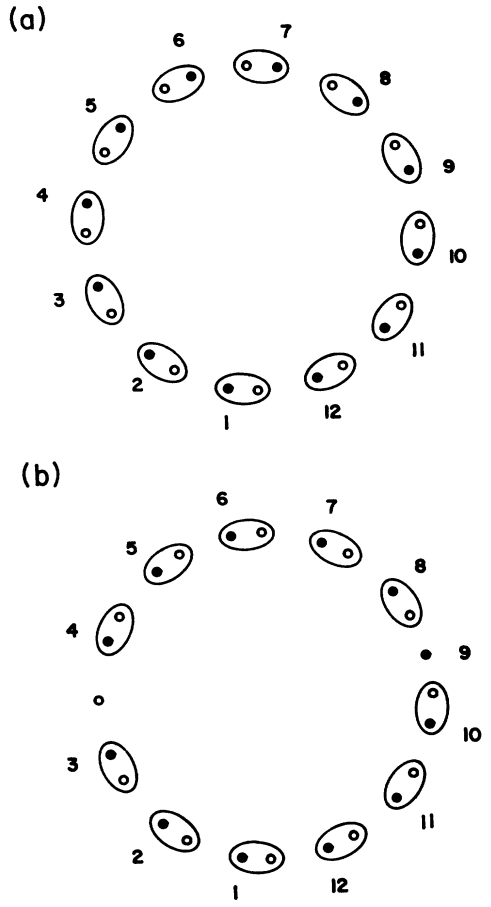

FIG. 9. Schematic representation of a HF polymer ring molecule formed by $N=12$ monomers. In (a) without and in (b) with a sharp kink-antikink pair. Black (white) circles represent fluorine (hydrogen) atoms and the monomer units are shown by enclosing a HF pair in an ellipse. It is seen that the introduction of the kink-antikink pair generates a well separated pair of a hydrogen and a fluorine atom, which are both not part of any monomer. Letting x_n be the shift of the nth fluorine atom away from the position in the middle between the two neighboring protons in counterclockwise direction we have in (a) $x_n=-x_{(0)}$, $n=1,\ldots,12$, whereas we have in (b) $x_n=x_{(0)}$, $n=1,2,3,10,11,12$, $x_n=-x_{(0)}$, $n=4,5,6,7,8$, and $x_9=0$. Here $x_{(0)}$ is the common optimum value of x_n of the undistorted system (a), and the numbering refers to that of the figure.

The on-site matrix elements $\varepsilon^{(i)}(x_{n-1},x_n,x_{n+1})$ contain a coupling between the nearest neighbors which we will relate to the electrostatic interactions. We write

$$\varepsilon^{(i)}(x_{n-1},x_n,x_{n+1})=\varepsilon_0^{(i)}(x_n)+Q(x_{n-1},x_n,x_{n+1}). \tag{10}$$

The last term is due to the potentials from the charges of the two neighboring monomers on site $n-1$ and $n+1$, respectively. Using the experimental[12] dipole moment and bond length of the isolated monomer quoted in Sec. III (1.80 D and 1.73 a.u., respectively) we will set $q=0.41e$ for the ground state of the polymer, i.e., for $x_n=x_{(0)}$. We will furthermore assume that q is proportional to x_n, although this is a very crude approximation. Nevertheless, the major purpose by including Q is to include a coupling between neighboring monomers and for that purpose the approximation is acceptable.

For the ground state of the polymer each monomer creates a dipole field. We will assume that for the excited states the electrostatic potentials only are caused by the dipoles, that only nearest neighbors need to be considered, that the potential on the nth monomer from the $(n-1)$th $[(n+1)$th$]$ monomer is a linear function of x_{n-1} $[x_{n+1}]$, that it is 0 for x_{n-1} $[x_{n+1}]=0$, and that it for x_{n-1} $[x_{n+1}]=x_{(0)}$ equals that of the monomer at a typically intermonomer distance of the solitonic excited polymer (which we will choose to be 4.6 a.u.). Then

$$Q(x_{n-1},x_n,x_{n+1})=-1.05\cos\alpha\,\frac{x_{n-1}-x_{n+1}}{x_{(0)}}\ \text{eV}. \tag{11}$$

We would like to point out that this is a very simplified model. But by comparing the results obtained without and with Q included we should be able to get some insight into the consequences of including electrostatic potentials.

We see that the potential Q is equal to 0 for the perfect chain [Fig. 9(a)]. For the solitonic excited chain [Fig. 9(b)] Q gives rise to a perturbation around the single kink.

For the perfect undistorted chain we have

$$x_n=x_0 \tag{12}$$

and the total electronic energy from (9) becomes

$$E_{TB}(x_0)=-2N\sum_{i=1}^{4}\varepsilon_0^{(i)}(x_0). \tag{13}$$

For the isolated monomer (i.e., $d_F\to\infty$, $N=1$) E_{TB} depends approximately exponentially on d_H [see Fig. 2(b)] and since $E_{TB}(x_0)$ of (13) is to be an even function of x_0 we will assume that

$$E_{TB}(x_0)=AN[1-\cosh(ax_0)]. \tag{14}$$

We will furthermore assume that each of the on-site

matrix elements $\varepsilon^{(i)}(x_0)$ have the same functional dependence (14), i.e.,

$$\varepsilon_0^{(i)}(x_0)=A^{(i)}[1-\cosh(ax_0)]. \tag{15}$$

The coefficients $A^{(i)}$ obey the constraint

$$2(A^{(1)}+A^{(2)}+A^{(3)}+A^{(4)})=A, \tag{16}$$

and we assume a to be independent of i. From the single-particle eigenvalue spectrum of the isolated monomer [Fig. 2(b)] as well as from the ionization potential of the polymer [Figs. 6(a) and 6(b)] this is seen to be reasonable.

In this model we have neglected constant shifts of the positions of the energies of the molecular orbitals such that the relative positions of the bands are not reproduced correctly. Only being interested in energy differences this is acceptable.

a and $A^{(i)}$ are determined from the calculations reported in the previous section, such that the total relative sum of the single-particle energies for each valence band is reproduced as well as possible.

The hopping integrals $t^{(i)}_{n,n+1}(x_n)\equiv t^{(i)}(x_n)$ are unimportant for the total energy of the perfect polymer but will be of importance for the total energy of the solitonic excited polymer and for the single-particle eigenvalue spectrum. We will assume that $t^{(i)}_{n,n+1}$ only depend on the hydrogen and molecular bond lengths of the nth proton and not on the neighboring bond lengths, i.e., only on x_n and not on x_{n+1}. They are even functions of x_n so we will expand them as

$$t^{(i)}(x_0)=t_0^{(i)}-t_2^{(i)}x_0^2, \tag{17}$$

where $t_0^{(i)}$ and $t_2^{(i)}$ are determined from the bandwidths $4t^{(i)}(x_0)$ for $x_0=0$ and $x_0=x_{(0)}$. The bandwidths of Figs. 6(c) and 6(d) indicate that such a dependence is justified.

To the attractive total tight-binding energy (9) we will add a repulsive term $E_{\rm rep}$. We will assume this to have a functional form similar to (14), i.e.,

$$E_{\rm rep}=\sum_{n=1}^{N}B[1-\cosh(bx_n)]. \tag{18}$$

B and b are determined from the conditions that the total energy per monomer of the perfect undistorted polymer

$$E_{\rm tot}(x_0)/N=[E_{\rm TB}(x_0)+E_{\rm rep}(x_0)]/N$$
$$=A[1-\cosh(ax_0)]+B[1-\cosh(bx_0)] \tag{19}$$

has a minimum at $x_0=x_{(0)}$ and reproduces the "dimerization" energy $E_{\rm dim}\equiv E_{\rm tot}(0)-E_{\rm tot}(x_{(0)})$.

With this we have introduced all the parameters entering the model.

We have modeled the polymer with a ring of $N=200$ monomers. In the first set of calculations we set

$$x_n=x_0 \tag{20}$$

and vary x_0 in the range 0 to $2x_{(0)}$ in order to check the computer codes and in order to obtain reference calculations for the perfect chain to compare the results for the solitonic excited chain with.

In the next set of calculations we set

$$x_n=x_{(0)}\tanh[(n-50.5-\delta)/L]\tanh[(n-150.0-\delta)/L]. \tag{21}$$

This corresponds to exciting a soliton-antisoliton pair, each of width L, at the positions $50.5+\delta$ and $150.0+\delta$. Due to the periodicity we have to have an even number of kinks plus antikinks. In general the widths of the soliton and antisoliton need not be the same but in order to simplify we here require them to be so. By varying δ the propagation of a soliton can be modeled. It should be pointed out that the form (21) corresponds to that proposed by Su, Schrieffer, and Heeger[43,44] for a soliton-antisoliton pair in *trans*-polyacetylene.

A special case is that of neglecting the coupling between neighboring monomers which corresponds to setting Q of Eq. (11) equal to 0. Then the model permits only integral values of δ, and the propagation is therefore to be considered as hopping. Therefore, we can in this case not examine the energy barriers for soliton propagation.

In Table I we list the parameters used in the calculations and some few key results. We have considered one route connecting the two degenerate minima keeping

TABLE I. The parameters used in examining the solitonic excitations of the hydrogen fluoride polymer. For the precise definitions, see the text. The table also gives the calculated equilibrium value of $x_{(0)}$, the "dimerization" energy $E_{\rm dim}$, and the creation energy of the soliton-antisoliton pair $E_{\rm sol}$ using the parameters of the table. Two sets of parameters—both derived from the first-principles calculations on the perfect undistorted polymer for fixed α—are reported; one for the zigzag structures ($\alpha=120°$) and one for the linear structures ($\alpha=180°$). For $\alpha=180°$ the parameters with superindex (3) or (4) are identical since they correspond to the double degenerate π_1 bands. As discussed in the text the results should be considered semiquantitative.

	$\alpha=120°$	$\alpha=180°$
A (eV)	1.30	0.41
a (bohr^{-1})	4.1	7.2
B (eV)	−0.64	−0.14
b (bohr^{-1})	5.1	10.1
$A^{(1)}$ (eV)	0.25	0.105
$A^{(2)}$ (eV)	0.16	0.100
$A^{(3)}$ (eV)	0.16	0.0
$A^{(4)}$ (eV)	0.08	0.0
$t_0^{(1)}$ (eV)	0.24	0.28
$t_0^{(2)}$ (eV)	0.84	1.85
$t_0^{(3)}$ (eV)	0.23	0.26
$t_0^{(4)}$ (eV)	0.23	0.26
$t_2^{(1)}$ (eV/bohr^2)	0.32	0.08
$t_2^{(2)}$ (eV/bohr^2)	0.57	1.52
$t_2^{(3)}$ (eV/bohr^2)	0.52	0.21
$t_2^{(4)}$ (eV/bohr^2)	0.27	0.21
$x_{(0)}$ (bohr)	0.475	0.246
$E_{\rm dim}$ (eV)	0.35	0.124
$E_{\rm sol}$ (eV)	0.35	0.124

$\alpha=120°$, and another route connecting the two degenerate short linear minima for fixed $\alpha=180°$. In this way we believe that the parameters have that large a spread that the results cover the whole range of possibilities. It should also be mentioned that by only including few significant figures in the parameters the model does not reproduce the results of Sec. III exactly but the differences should for the present purpose be unimportant.

For the special case of $Q=0$ our numerical calculations give that for $\delta=0$ the soliton-antisoliton pair with the lowest creation energy has $L\rightarrow 0$. This result is related to the small values of the hopping integrals $t^{(i)}(x)$. Neglecting them the total energy becomes

$$E_{\text{tot}} \simeq A \sum_{n=1}^{N} [1-\cosh(ax_n)] + B \sum_{n=1}^{N} [1-\cosh(bx_n)]. \tag{22}$$

The soliton induces at least one n value for which $x_n=0$. Denoting this value l, (22) can be rewritten as

$$E_{\text{tot}} \simeq A \sum_{\substack{n=1 \\ n\neq l}}^{N} [1-\cosh(ax_n)] + B \sum_{\substack{n=1 \\ n\neq l}}^{N} [1-\cosh(bx_n)], \tag{23}$$

which is smallest for $|x_n| = |x_{(0)}|$ for $n\neq l$. The soliton-antisoliton pair creation energy E_{sol} is then

$$E_{\text{sol}} \simeq -A[1-\cosh(ax_{(0)})] - B[1-\cosh(bx_{(0)})], \tag{24}$$

which is the "dimerization" energy E_{dim}. By including the nearest neighbor interactions $t^{(i)}(x)$ as a perturbation these results are only modified slightly.

When including the dipole potentials (11) it turns out that the soliton-antisoliton pair with the lowest creation energy still has $L\rightarrow 0$ and that for this value E_{sol} is unchanged. This is understandable since Q introduces only weak couplings between the x_n's.

That E_{sol} is comparable to E_{dim} is different from the results for *trans*-polyacetylene where E_{sol} is typically found[43,44] to be one order of magnitude larger than E_{dim}. The distortions of the polymer geometry upon dimerization for *trans*-polyacetylene are however much smaller compared with those of hydrogen fluoride, which might cause the differences in the energies.

For *trans*-polyacetylene the simplest model[43,44] predicts that the soliton induces a state in the middle of the gap. This can be interpreted as due to the soliton leading to an unpaired electronic orbital with a zero total interaction with the rest of the polymer. A similar interpretation for HF would give that the soliton leads to states, each above the energies of the band from which it is derived.

We will first discuss the special case of vanishing Q. Then the soliton induces states slightly above the valence bands as predicted. They are for $\alpha=120°$ placed 0.4 eV (σ_1), 0.1 eV (σ_2), 0.3 eV (σ_3), and 0.1 eV (π_1) above the top of their respective valence bands. For $\alpha=180°$ the corresponding values are much smaller, 0.04 eV (σ_1), 0.02 eV (σ_2), and 0.0 eV (π_1), because of the smaller value of $x_{(0)}$. When increasing L these numbers increase, and also more levels are moved out from the ranges of the valence bands. E.g., for $\alpha=120°$ and $L=5$ we find for each valence band 5–11 levels up to 0.7 eV (σ_1), 0.5 eV (σ_2), 0.6 eV (σ_3), and 0.3 eV (π_1) above the valence band edges. This can be understood as a result of the larger L generating locally a structure with an effective smaller constant $x_n=x_0$ than that of the rest of the polymer. The energy levels of this subsystem appear therefore above those of the rest of the system [cf. Eq. (15)]. It is interesting to notice that for the π_1 orbitals for $\alpha=180°$ $A^{(i)}=0$ and the soliton with $L=5$ therefore induces two states symmetrically placed 0.1 eV above and below the band. This is the only state for which such a feature was found.

For the larger L the more occupied states above the band edges lead to an increase in the tight-binding part of the total energy. This is partly compensated by an accompanying decrease in the repulsive part but the total energy is increased. In our case the creation energy for the soliton with $L=5$ is roughly 5 eV. It should be mentioned that for $L=5$ the soliton is so delocalized that a continuum description might be justified, and our results can hence be compared with those of continuum models.

For a given geometry of the nuclei, neglecting spin, and only considering a single energy band, the electronic eigenvalue problem

$$\left[\sum_n [-t_{n,n+1}(c_n^\dagger c_{n+1}+c_{n+1}^\dagger c_n)+\varepsilon_n c_n^\dagger c_n]\right]\sum_n x_n \mid c_n\rangle = e\sum_n x_n \mid c_n\rangle \tag{25}$$

can be transformed into the scattering problem (see, e.g., Ref. 46 for a similar treatment of the conjugated polymers)

$$\begin{bmatrix} x_{n+1} \\ x_n \end{bmatrix} = \underline{T}_n \begin{bmatrix} x_n \\ x_{n-1} \end{bmatrix} \tag{26}$$

with

$$\underline{T}_n = \begin{bmatrix} (\varepsilon_n - e)/t_{n,n+1} & -t_{n-1,n}/t_{n,n+1} \\ 1 & 0 \end{bmatrix}. \tag{27}$$

For a soliton which changes the molecular bond lengths of the monomers $-l,-l+1,\ldots,l-1,l$ and leaves the rest unchanged we have

$$\underline{T}_n = \underline{T} = \begin{bmatrix} (\varepsilon - e)/t & -1 \\ 1 & 0 \end{bmatrix} \tag{28}$$

for $n<-l$ and $n>l+1$ when neglecting the electrostatic term Q. The conditions for the soliton to induce a state localized around $n=0$ are that it corresponds to an eigenvalue $\lambda_>$ of $\underline{T}$ with modulus larger than 1 for $n<l$ and to an eigenvalue $\lambda_<$ of $\underline{T}$ with modulus smaller than 1 for $n>l+1$. Then

$$\underline{T}_{l+1}\underline{T}_l \cdots \underline{T}_{-l} \begin{bmatrix} \lambda_> \\ 1 \end{bmatrix} = c \begin{bmatrix} \lambda_< \\ 1 \end{bmatrix}, \tag{29}$$

where $(\lambda,1)$ are the corresponding eigenvectors of $\underline{T}$ and

c is a constant. The eigenvalues of $\underline{T}$ are

$$\lambda=\frac{\varepsilon-e}{2t}\pm\left[\left[\frac{\varepsilon-e}{2t}\right]^2-1\right]^{1/2}, \tag{30}$$

so in order to have two different moduli we must have

$$e>\varepsilon+2t \quad \text{or} \quad e<\varepsilon-2t, \tag{31}$$

i.e., that the energy of the state is outside the range of the band. In order to determine the final position of the state one must solve Eq. (29). In general this becomes a $(4l+4)$th order equation in the energy e. Only for the sharp kink ($l=0$) this is manageable but still tedious. Including the extra term Q corresponds to replacing l by $l+1$.

The lowest conduction band orbitals are formed by molecular antibonding orbitals of the monomers. Therefore, the $A^{(i)}$ parameter for these states will be negative and the soliton induced state will appear below the conduction band edge. However, inclusion of Q might modify this. In total the soliton will lead to a decrease in the gap but the decrease will be so small that it will be of little practical importance.

When including the dipole potentials (11) but keeping $L\rightarrow 0$ some shifts in the single-particle energy spectrum show up, although as mentioned above the total energy is unchanged. The shifts should be expected because of the local electrostatic potentials close to the kink. Our calculations give that for $\alpha=120°$ the soliton-antisoliton pair induces states 0.6 eV and 0.9 eV below and 0.2 eV, 0.2 eV, and 1.4 eV above the σ_1 band; 0.8 eV below and 0.9 eV above the σ_2 band; 0.7 eV and 0.9 eV below and 0.3 eV, 0.3 eV, and 1.3 eV above the σ_3 band; and 0.6 eV and 0.9 eV below and 0.1 eV, 0.2 eV, and 1.0 eV above the π_1 band. The appearance of more states is in agreement with the discussion above. Also for $\alpha=180°$ we find that more states are moved out from the band region and that the shifts in general are 1–5 times larger compared with the results for vanishing Q. Thus, inclusion of Q leads to states both below and above the bands, in contrast to the results for $Q=0$ and for *trans*-polyacetylene.

In a continuum description of the energy of a soliton Jansen *et al.*[32] have obtained a larger value for the creation energy of a single soliton for HF, 1–3 eV. However, they fixed not only α but also d_F and this will lead to an overestimate of E_{dim} and hence also of E_{sol}. Furthermore, as our results as well as their results indicate the region deformed by the soliton is so small that the continuum approximation might not be justified.

Pietronero[47,48] has within the CNDO approximation examined proton motion in cyclic HF hexamers. He calculated the total energy as a function of the position of one proton when keeping the positions of all the other five and of the six fluorine atoms fixed. For $d_F=4.71$ a.u. his results show that the energy per monomer of the structure with all protons in the symmetric position ($d_H=d_F/2$) is 0.6–0.7 eV above that of the ground state. This energy is about twice our E_{dim} with which it should be compared. Also for d_F fixed at 4.71 a.u. but for the infinite linear polymer ($\alpha=180°$) Karpfen and Schuster[49] report an *ab initio* Hartree-Fock value of 0.55 eV. However, when keeping d_F fixed at 4.80 a.u. we find a value of 0.52 eV for $\alpha=120°$ and 0.45 eV for $\alpha=180°$ in good agreement with the results of Pietronero[47,48] as well as with those of Karpfen and Schuster[49] indicating that there is a considerable ($\sim 50\%$) energy gain by allowing d_F to relax. Pietronero[47,48] reported that the structure with one proton at the symmetric position and the others kept fixed at their ground state positions has a total energy about 1.5 eV above that of the ground state—much larger than our E_{sol} (this structure is in our model equivalent with that of a soliton with $L\rightarrow 0$ from a total energy point of view). This is surprising since from the discussion above and from that of Sec. IV A it would be expected that the CNDO method reproduces correctly the energies for bent structures. However, it turns out that for d_F kept fixed at 4.35 a.u., all d_H's except for one set to 1.89 a.u., and the last proton at the symmetric position the excited state thereby created has a total energy lower than that of the ground state, so we believe that the absolute numbers of Pietronero should be taken with some caution.

Our model indicates that upon exciting a soliton the length of the polymer is changed. This seems not fully justified and one could impose the restriction of fixed chain length. This condition would lead to a correlation between the position coordinates x_n and/or to leaving the constraint of constant α for all unit cells. We believe that the resulting more complicated model will give results only quantitatively but not qualitatively different from those presented in this section.

Furthermore, the electrostatic interactions which we only have considered approximately could be included in a more proper way. But also in this case we believe that our major findings will not be changed.

VI. PHONONS

The total energies of Fig. 4 can be expanded to second order in the bond lengths around their equilibrium values thus defining a force field in which the nuclei move. From this force field we can determine the frequencies of the frozen phonons for the stretch modes for the zone center phonons. The Brillouin zone is defined as being that corresponding to the helical symmetry of the single chain as in detail described by Higgs[50] and Piseri and Zerbi.[51]

In order to get the full dispersion curves of the frozen phonons one has to increase the size of the unit cell and simulate the displacement pattern of a phonon for a k of a lower symmetry. This procedure has in detail been discussed by, for instance, Kunc and Martin[52] for the case of solid GaAs. As discussed by these authors the phonons considered in this section will lead to long-range electrostatic fields which will change the frequencies. This effect is however relatively small and we will neglect it here.

By denoting the force constants for the molecular and hydrogen bond f_1 and f_2, respectively, the optical B_1 stretch phonon frequency at the zone center becomes

$$\omega=[(f_1+f_2)/\mu]^{1/2}, \tag{32}$$

with μ being the reduced mass of the single monomer.

Assuming that the total energies for $\alpha=120°$ sufficiently well describe those for the optimum α ($=125°$)

we obtain $\omega=3535$ cm^{-1} for HF and $\omega=2561$ cm^{-1} for DF, i.e., a shift of 8.5% and 10.0%, respectively, compared with the vibrational frequencies of the isolated monomers reported in Sec. III. A similar shift has been observed experimentally by Lisy *et al.*[53] in vibrational spectra when passing from $(HF)_3$ to $(HF)_6$. The shift is related to the larger molecular bond lengths in the polymer, and to the protons being connected with bonds in two opposite directions in the polymer whereas it only is under the influence of one bond in the monomer. (We will in this section use the word proton for both the hydrogen nucleus and the deuterium nucleus.)

From infrared (ir) spectroscopy Kittelberger and Hornig[54] obtained the frequencies 3404 and 2526 cm^{-1} for the two polymers in excellent agreement with our results. Also the Raman spectroscopy result by Anderson *et al.*[55] (3386 and 2511 cm^{-1}) and the ir data of Desbat and Huong[56] (3360 and 2460 cm^{-1}) agree well with ours.

Model calculations using parametrized force fields by Tubino and Zerbi[57] gave 3404 and 2526 cm^{-1} for the two polymers, respectively, whereas those by Tse and Chang[58] gave 3306 cm^{-1} for HF. Finally, Higgs *et al.*[59] obtained 3317 cm^{-1} for HF.

From the *ab initio* Hartree-Fock calculations on the polymer Beyer and Karpfen[29] calculated the frequencies to be 4170 and 3023 cm^{-1}, respectively. As for the monomer the Hartree-Fock method overestimates the frequencies. It is surprising to notice that they found the largest basis set to give the largest overestimates.

Trying to use the total energies of Fig. 4(a) to describe a force field which should be applied to the whole Brillouin zone did not work: the width of the band was found to be roughly 100 cm^{-1}, whereas it experimentally was determined to be 200–300 cm^{-1} wide.

Axmann *et al.*[60] have reported an experimental root mean square thermal amplitude for the proton in solid HF at 175 K of 0.87 a.u., assuming the amplitude to be isotropic. This value is so large that the anharmonicities and the existence of the second degenerate minimum become non-negligible. In the harmonic approximation a phonon is an excitation from an energy $\frac{1}{2}\hbar\omega$ to $(n+\frac{1}{2})\hbar\omega$. Thus the energy of the first excited state for the $k=0$ stretch phonon is 0.66 eV for HF and 0.48 eV for DF, i.e., above the barrier for a collective shift of all the protons (see Sec. IV). Thus, the harmonic approximation is questionable. We will therefore now consider a simple model which includes anharmonicities.

First of all we notice that the frequency (32) is that of an isolated dimer with a reduced mass μ and an effective spring constant $f=f_1+f_2$. Therefore, we will consider the effect on the single-particle eigenvalues when including anharmonicities in this potential, and thereby neglecting couplings between the neighboring protons (i.e., assuming the mode to have no dispersion). The system then becomes equivalent with the FHF^- molecular ion, which has been discussed, for instance, in Ref. 61. We will assume the potential to be a sum of two Morse potentials, i.e.,

$$V(x)=D\{1-\exp[-\beta(x_s-x)]\}^2 + D\{1-\exp[-\beta(x_s+x)]\}^2, \tag{33}$$

where $x=0$ corresponds to the saddle point ($d_H=d_F/2$). The constants D, β, and r_s are determined from the conditions that the potential reproduces the correct barrier height, minima, and curvature at the minima, i.e.,

$$\begin{aligned} &V(0)-V(\pm x_0)=V_0, \\ &V'(\pm x_0)=0, \\ &V''(\pm x_0)=f. \end{aligned} \tag{34}$$

By choosing the form (33) for the potential we can fulfill all the conditions (34) and simultaneously obtain a reasonable form of the potential. With $V(x)$ being a polynomial we would either not be able in general to fulfill all conditions (34) or introduce extra artificial local extrema.

In total we end up with the one-dimensional Schrödinger equation

$$\left[-\frac{1}{2\mu}\frac{d^2}{dx^2}+V(x)\right]\psi(x)=E\,\psi(x). \tag{35}$$

As is common practice (see, e.g., Ref. 61) we solve this numerically by expanding $\psi(x)$ in the eigenfunctions of the harmonic oscillators, i.e., in the set of functions (in a.u.)

$$u_n^{\pm}=(n!2^n)^{-1/2}(\mu\omega/\pi)^{1/4}h_n[(\mu\omega)^{1/2}(x\pm x_0)] \times\exp[-\mu\omega(x\pm x_0)^2/2], \tag{36}$$

with ω given by (32) and h_n being the nth Hermite polynomial. These functions are the exact solutions to (35) with $V(x)$ being replaced by the harmonic potential

$$V(x)=\tfrac{1}{2}f(x\pm x_0)^2. \tag{37}$$

The Hamiltonian and overlap matrices can easily be calculated numerically by Gauss integration and by using that the basis functions are eigenfunctions to the Schrödinger equation (35) with the potential given by (37). Diagonalizing gives the eigenvalues and eigenvectors.

The computer codes and the numerical integration were tested by considering the potential (37) with basis functions up to between $n=5$ and $n=9$ included on either site. The results were converged to ±2 cm^{-1} in this case.

We then considered the potential (33) where x_0 was set equal to $d_F/2-d_H$ for the local minimum for $\alpha=120°$ in Fig. 4(a), i.e., $x_0=0.51$ a.u. We considered two barrier heights: one corresponding to keeping d_F and α constant (0.52 eV; the high-barrier case), and another corresponding to the smallest possible barrier for α constant (0.30 eV; the low-barrier case). The results should thus cover the possible outcomes of an experiment. Since $f=1.23$ eV/bohr^2 we find $D=0.298$ eV, $\beta=5.23$ a.u., and $x_s=0.523$ a.u. in the high-barrier case, and $D=0.160$ eV, $\beta=6.64$ a.u., and $x_s=0.515$ a.u. in the low-barrier case.

In Table II we give the results for HF and DF. The excitation energies are all relative to the ground state energy. It turned out that by including $n=8$ basis functions the results were well converged.

Both the ground state and the first excited state are in

TABLE II. Excitation energies in cm^{-1} for HF and DF assuming a proton double-well potential. The numerical uncertainties are estimated to be 10 cm^{-1}. Also given are the values obtained using the harmonic approximation. These values are indicated with an asterisk. For further details, see the text.

HF		DF	
High-barrier	Low-barrier	High-barrier	Low-barrier
370	565	90	200
1955	2045	1250	1135
3850	4070	2205	2225
3535*	3535*	2561*	2561*

all cases mainly formed by $n=0$ basis functions. From proton $n=0$ basis functions centered in each of the two half-parts of the double-well symmetric and antisymmetric linear combinations are formed. The latter is slightly above the former in energy, the difference being larger for lighter particles and smaller barriers as seen in the table. The calculations furthermore give that the most delocalized function has the smallest $n=0$ components, i.e., the symmetric ground state function for HF in the low-barrier case.

Since the energies of the first excited state correspond for DF to a temperature of some few hundred K both these states can be important from a statistical point of view.

For $k=0$ absorptions in the range 350–550 cm^{-1} for HF and in the range 50–200 cm^{-1} for DF have been observed.[54] These broad-peak absorptions are ascribed several other vibrations but can accordingly also be related to the proton tunneling.

The third excitation energy is in reasonable agreement with the frequencies calculated above using the harmonic potential, when noticing the crudeness of the model. The state is mainly an antisymmetric combination of the $n=1$ and $n=2$ basis functions.

The second excitation energy is found in a region where to our knowledge no absorption has been observed. It corresponds to a state which is a mixture of all basis functions, thus being the excitation energy which converged most slowly of them all, and furthermore being quite delocalized. Therefore, some adjustments in the energy can be expected due to slower convergence as a function of the basis set size and due to coupling to neighboring sites in the polymer. Since this state has a quite different shape than that of the ground state we will expect the Raman and ir cross sections to be small, thus making it difficult to observe experimentally.

That the energy spectrum changes much upon including anharmonicities is not surprising. With the parameters for the Morse potential (33) the anharmonic term $n(n+1)\omega_e hcx_e$ of (8) is for HF in the high-barrier case for a single Morse potential comparable with the harmonic term $n\omega_e hc$ already for $n=1$. Furthermore, the single Morse potential possesses in all cases only one bound state, except for DF in the high-barrier case where there are two bound states. Therefore, the excited states for the full potential (33) will be delocalized over the whole double-well region.

Our finding of the second excited state between those found in the pure harmonic approximation is in accordance with the results of Brickmann and Zimmermann.[62] They examined the proton eigenfunctions in symmetric as well as asymmetric double-well potentials with $V(x)$ being a fourth order polynomial. They also considered the case of adding a potential formally written as

$$T=\lim_{A\to\infty} A\delta(x) \tag{38}$$

in which case the eigenstates are those of a single well. For a symmetric potential with a barrier height (without T) of 7000 cm^{-1} = 0.87 eV and $x_0=0.57$ a.u. they found, when including T, two energy levels (the ground state and the first excited state) for energies below the barrier height and a third level (the second excited state) well above the barrier. Omitting T the first excited level was split into two. For the second excited level one level was roughly not shifted whereas the other was placed approximately in the middle between the unshifted level and the positions of the first excited states. Comparing with our results it is more reasonable to compare their first excited state with our ground state, since their ground state is so deep lying in energy that it does not feel the anharmonicity as much as ours does. Accordingly, a correspondence between their $(n+1)$th level and our nth level can be made, and the results are then in qualitative agreement.

VII. MODEL POTENTIALS FOR LIQUID AND GASEOUS HF

As mentioned in the Introduction both gaseous and liquid hydrogen fluoride consist to a large part of clusters of HF monomers. Nevertheless, many theoretical examinations of the dynamics of the gas and the liquid take as their starting point the isolated dimer. From *ab initio* calculations on the dimer model potentials are derived which then are assumed appropriate for the dynamical properties. Obviously these models neglect "multimer" effects beyond dimers. Here, we will examine how well some few of these model potentials describe the total energies found for the polymer. The discrepancies are then to some extent to be ascribed multimer effects which should be included in improved models. We will examine a single model potential for HF vibrational relaxation in the gas phase,[63] and a few for describing the dynamics of liquid HF.[64–70] More sophisticated model potentials than those have later been proposed[71–73] and we will compare our results with the results of one of those.

Poulsen *et al.*[63] examined theoretically the energy transfer in the HF + HF system. They fitted *ab initio* Hartree-Fock total energies for the dimer calculated by Yarkony *et al.*[13] for a large number of configurations of two rigid monomers (i.e., the monomer bond lengths were kept fixed). With R being the distance between the center of mass of different monomers their potential was

$$V=V_{\text{Coulomb}}+V_{\text{SR}}-\frac{C_6}{R^6}, \tag{39}$$

with V_{Coulomb} being electrostatic potential between point

charges $\pm q$ on the nuclei, and V_{SR} a short-range potential written as pair potentials

$$V_{SR} = V_{HH} + V_{FF} + V_{FH} + V_{HF}. \quad (40)$$

Here, V_{HF} and V_{FH} were of the Morse potential form, V_{HH} an inverse power, and V_{FF} a combined exponential and inverse power; all as functions of the interatomic distances. Since they were interested in energy transfers they had to include an intramonomer potential which they assumed to be of a corrected harmonic oscillator form. Since the precise form of it was not given we will not include it here.

Also Klein *et al.*[64] fitted the total energies of Yarkony *et al.*[13] to a model potential. In order to describe the dipole as well as the quadrupole moment of the isolated monomer they modeled the electrostatic interactions by assuming three charges per monomer, $+q$ on each of the nuclei and $-2q$ on a point somewhere on the molecular axis. Since they were interested in simulating the dynamics of the liquid they assumed the monomers to be rigid. Besides the Coulomb interactions they included short-range intermonomer potentials of the form (40). V_{HH} was an exponential, V_{HF} and V_{FH} of the Morse potential form, and V_{FF} a combined exponential and inverse power.

In another paper McDonald and Klein[65] fitted the *ab initio* Hartree-Fock total energies of Yarkony *et al.*[13] with a slightly different model potential. The most important difference was that the Coulomb interactions were described assuming only two point charges per monomer, $\pm q$ on the nuclei. The short-range interactions were slightly modified. As above the monomers were assumed rigid.

Jorgensen and Cournoyer[66–68] have performed *ab initio* Hartree-Fock calculations on the dimer with rigid monomers. They considered two different basis sets, the so-called 6-31G[66,67] and the so-called STO-3G[68] basis, both of which correspond to expanding Slater-type orbitals in Gaussians. The results were fitted with electrostatic potentials from point charges, either two[66,67] or three[68] per monomer. The short-range interactions were all described by inverse powers.

In Refs. 64–68 the potentials were used in describing the dynamics of the liquid. The different potentials, except for that of Ref. 68, have been compared and discussed by Klein and McDonald[69] and the reader is referred to that paper for a more detailed discussion of those models.

A much simpler intermonomer potential between rigid monomers has more recently been proposed by Cournoyer and Jorgensen.[70] A three charge per monomer model ($+q$ on the nuclei, $-2q$ somewhere on the bond) was used in describing Coulombic interactions, and the short-range interactions were simplified to a single Lennard-Jones potential between the fluorine atoms.

All of these models just described were derived from *ab initio* Hartree-Fock calculations on the dimer consisting of two rigid monomers. Therefore, per definition they do not contain any correlation effects, and the description of the intra-monomer potential is either completely lacking or quite approximative.

A more detailed analysis has been undertaken by Redmon and Binkley.[72] They calculated total energies for the dimer using the *ab initio* Hartree-Fock method where parts of the correlation effects were taken into account by fourth order Møller-Plesset perturbation theory. Furthermore, they considered different molecular bond lengths thereby leaving the rigid monomer approximation. The results were fitted with a quite complicated expression containing roughly 100 parameters (in contrast to the other models just described which each have roughly 10 parameters).

The potential was assumed to have the form

$$V = V_{\text{Coulomb}} + V_{\text{LEPS}} + V_3 + V_4 + V_{\text{disp}}. \quad (41)$$

V_{Coulomb} was the electrostatic potential arising from two point charges per monomer as, e.g., Poulsen *et al.*[63] considered.

V_{LEPS} was written as a function of the so-called Coulomb and exchange integrals Q_{ij} and J_{ij} (i and j labeling atoms). In using the potential for the polymer one has to be careful since V_{LEPS} contains both intra- and intermonomer contributions. Therefore, V_{LEPS} is to be modified such that the intramonomer contribution is only counted once per monomer.

V_3 and V_4 were three-body and four-body potentials, respectively. Since their calculations only considered the dimer the three (four) sites of V_3 (V_4) were restricted to belonging to two monomers, and three- and four-body interactions for atoms of more monomers were lacking.

Although the potential was used in a subsequent work by Schwenke *et al.*[74] in examining energy transfers in the HF + HF system, the parameters given by Redmon and Binkley[72] are erroneous, such that, e.g., the Coulomb and exchange integrals for FF interactions diverge as a function of interatomic distances. Changing a sign, thereby making them convergent does not lead to reasonable results. Therefore, we did not consider this potential in our analysis of the model potentials. (See, however, the *Note added.*)

Murad *et al.*[71] proposed a model where the anisotropy of the polarizability of the monomers was included. However, only a few details were given, so this potential is also excluded from our analysis.

Finally, Spackman[73] proposed a simple model in which the monomers were assumed rigid. He included short-range interactions consisting of a repulsive term written as exponentials and an attractive dispersion term written as R^{-6} terms. The parameters entering these potentials were given in another paper.[75] He argues that the repulsive term should be omitted for the two atoms forming a hydrogen bond. In order to get reasonable results we concluded that the dispersion term should also be omitted in this case. He considered electrostatic interactions between atom centered charges and multipoles. The values of the charges and multipoles were determined by partitioning charge densities of the monomer into atomic parts, where the charge densities were obtained from *ab initio* Hartree-Fock calculations of Cade and Huo.[76] Since we are only interested in the electrostatic interactions between well-separated monomers we will model his atomic monopole, dipole, quadropole, octopole, and hex-

adecapole by five equidistant point charges placed on a line passing through both atoms of the monomer, and with the middle one placed on the atom of interest. With δ being the distance between the point charges the values of the point charges are determined from

$$\sum_{i=-2}^{2} (i\delta)^l q_i = \mu_l, \quad l=0,1,2,3,4, \tag{42}$$

where μ_l is the value of the 2^l pole of the atom of interest. We considered both $\delta=0.2$ a.u. and $\delta=0.05$ a.u. and found only minor differences indicating that it is justified to model the atomic mono- and multipoles by point charges.

It should be pointed out that this model, although it includes more terms, differs only a little from the more simple ones mentioned in this section. The main difference is the more complicated electrostatic interactions, but there are no attempts to include the interactions between the molecular orbitals.

We have calculated the total energy per monomer as a function of the fluorine fluorine nearest neighbor distance d_F for the zigzag and the linear polymer using these model potentials. The long-range electrostatic interactions were calculated by including all terms up to tenth nearest neighbor interactions, whereas for the short-range interactions we only included up to second nearest neighbors. Although most of the models consider rigid monomer with molecular bond lengths d_H equal to those of the isolated monomers we have chosen to consider three values of d_H: 1.70 a.u. which is close to the value of the

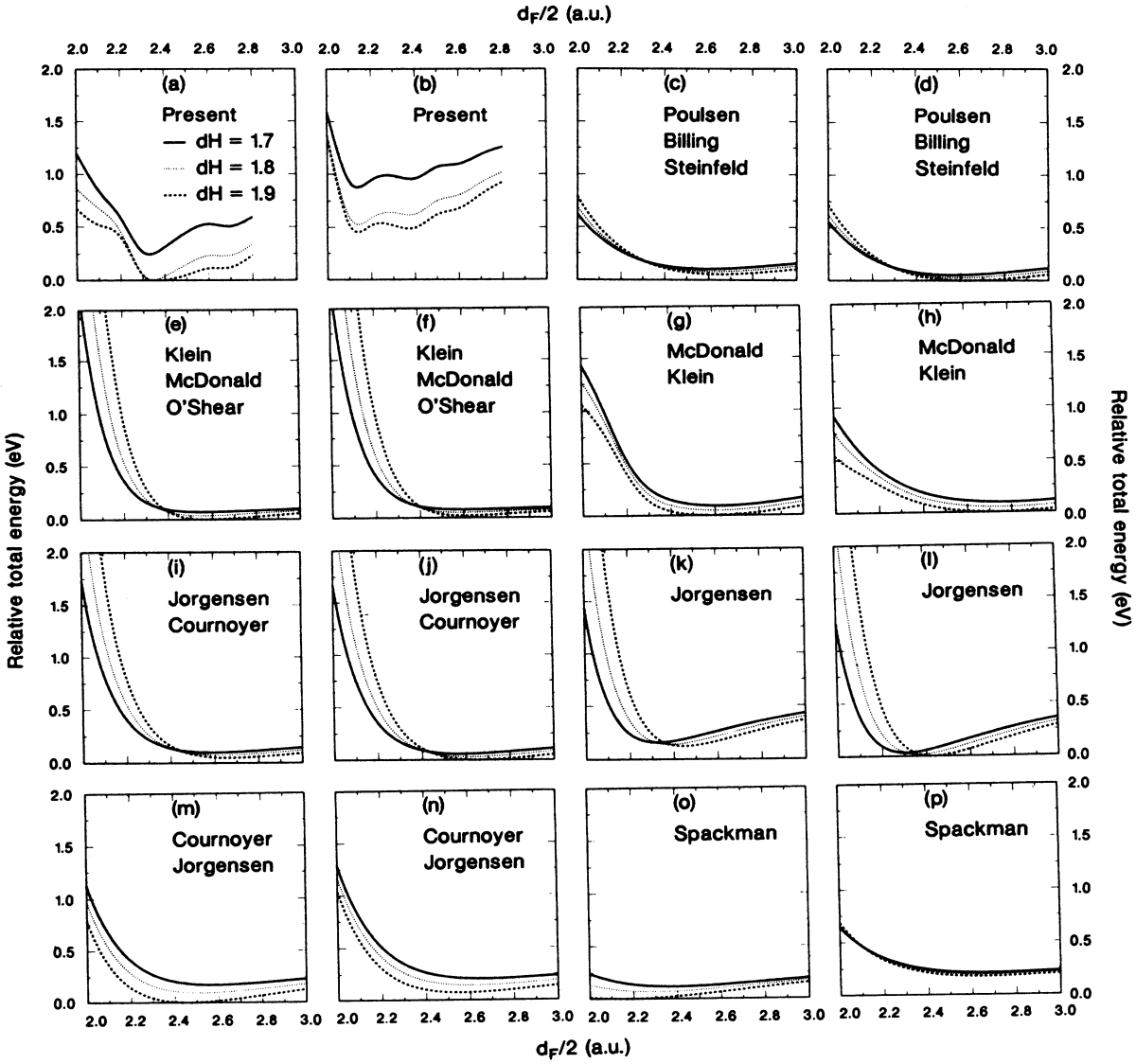

FIG. 10. Relative total energy in eV as a function of half the fluorine fluorine distance $d_F/2$ for three values of the molecular bond length d_H ($d_H=1.7$ a.u., solid curves; $d_H=1.8$ a.u., dotted curves; $d_H=1.9$ a.u., dashed curves) for zigzag [(a), (c), (e), (g), (i), (k), (m), and (o)] and linear [(b), (d), (f), (h), (j), (l), (n), and (p)] polymers. The results of the first-principles calculations [(a) and (b)] are compared with those predicted by the model potentials of Ref. 63 [(c) and (d)], Ref. 64 [(e) and (f)], Ref. 65 [(g) and (h)], Refs. 66 and 67 [(i) and (j)], Ref. 68 [(k) and (l)], Ref. 70 [(m) and (n)], and Ref. 73 [(o) and (p)]. Each pair of figures has the same common zero of energy for both zigzag and linear structures.

isolated monomer, 1.90 a.u. which is close to the optimal value of the polymer, and 1.80 a.u. as an intermediate value. In Fig. 10 we show the resulting total energies as a function of $d_F/2$ together with those extracted from our first-principles calculations of Fig. 4. For each model potential the results are shown relative to the lowest energy calculated for the described range of d_H and d_F for both zigzag and linear structures.

Our first-principles results [Figs. 10(a) and 10(b)] show for both zigzag and linear structures a small local maximum for $d_F/2 \simeq 2.5-2.6$ a.u. This we believe to be a consequence of the unusually strong hydrogen bond of hydrogen fluoride: When pulling the monomers apart the molecular bond lengths increase so that as a function of fixed $d_F/2$ the optimum value of d_H shows a maximum of 1.93 a.u. (1.96 a.u.) for $d_F/2 = 2.7$ a.u. (2.6 a.u.) for the zigzag (linear) structures. These local maxima manifest themselves as the oscillations in Figs. 10(a) and 10(b). Unfortunately, the parameter-free calculations by Jansen *et al.*[32] allow us not to compare this result with their results. Comparing now with the model potentials we see that none of them show this feature, which, however, is not surprising, since they all consider the monomers to be rigid with bond lengths as that of the isolated monomers. Since the elongation of the molecular bond is up to 15% we find the rigid monomer approximation not to be fully justified for HF with its strong hydrogen bond. Furthermore, *ab initio* Hartree-Fock calculations[77] on the dimer yielded an elongation of the molecular bond of only 0.5%, whereas the *ab initio* Hartree-Fock calculations by Swepston *et al.*[78] gave an elongation of 1–2 % for the trimer, which is slightly larger than that found by Liu *et al.*[79] For the tetramer Liu *et al.* find an elongation twice that of the trimer. However, Clark *et al.*[80] did not find any elongation for the tetramer from their *ab initio* Hartree-Fock calculations. Since the crystal structure of HF clearly gives a longer molecular bond than that of the single dimer, this is a point where "multimer" effects clearly are recognized, but where it might be difficult for parameter-free methods to reproduce this trend, such that theoretical energy surfaces for defining new model potentials might be difficult to obtain.

In Fig. 10 we see that all the model potentials in which only two point charges per monomer are included find the linear chain to have lower energy than the zigzag chain [Figs. 10(c), 10(d), and 10(i)–10(l)] or almost the same energy [Figs. 10(g) and 10(h)]. With three or more point charges per monomer the zigzag structure is correctly predicted to have the lowest energy [Figs. 10(e), 10(f), and 10(m)–10(p)]. This is in agreement with the results for the dimer (see, e.g., Ref. 81).

The energy difference between zigzag and linear structures is found to be considerably smaller than what we predict with the model by Spackman [Figs. 10(o) and 10(p)] giving the best agreement with our results. Since the energy difference mainly is due to differences in long-range interactions and since these interactions are those which Spackman has considered in more detail we believe these to be improperly described by the other model potentials. This will also affect the hydrogen bond energy of the polymer compared with that of the dimer. Redington[81] has shown that for one of the better model potentials [Ref. 64; Figs. 10(e) and 10(f)] this energy increases with only 20–25 % in contradiction to the results reported in Sec. IV A.

For the dimer the experimental value of $d_F/2$ is 2.64 ± 0.05 a.u.,[82] which is roughly 10 % larger than that of the polymer. In Fig. 10 we see that many of the model potentials [Figs. 10(c)–10(j)] are not able to describe this decrease. On the other hand, Spackman's model [Figs. 10(o) and 10(p)] predicts a substantial decrease in the $d_F/2$. By excluding his very large atomic hexadecapoles (and thereby only having four point charges per atom) the interatomic distance became in much better agreement with ours.

Many of the model potentials predict a shift in the optimum d_H value around the optimum $d_F/2$ value [Figs. 10(c)–10(f) and 10(i)–10(l)]. This is in contrast to the first-principles results of Figs. 10(a) and 10(b).

Finally, the results of Figs. 10(c)–10(p) predict hydrogen bond energies ranging from 0.27 to 0.65 eV for d_H fixed at 1.7 a.u. changing to from 0.30 eV to 0.68 eV for d_H in the range 1.7–1.9 a.u. The best agreement with the first-principles results of Sec. IV A is obtained with the potential by Jorgensen [Figs. 10(k) and 10(l)], which intuitively is clear from the figure. We believe that there are two main reasons for this general discrepancy. First of all, none of the considered model potentials includes a detailed description of the interaction between the molecular orbitals of the monomers, which we in Sec. IV C found to be important. Secondly, the models neglect dielectric screening, which, however, must be important for these materials in order to get nondiverging macroscopic electric fields. The dielectric constant should be changed such that $4\pi\epsilon > 1$ a.u., and the electrostatic interactions become then of shorter range.

Recently, Honda and Kitaura[83] have proposed a model which takes the interaction between the molecular orbitals into account. This interaction is written as parametrized functions of the overlaps between the molecular orbitals, but where these overlaps on the other hand have to be calculated. In addition to this they included electrostatic interactions between two point charges per monomer. The monomers were assumed rigid. It is interesting to notice that their binding energy and geometry of the dimer are in excellent agreement with experimental values in contrast to all other model potentials using only two point charges per monomer. This we believe to be a further indication of the importance of the interaction between the molecular orbitals and we find their model promising for further developments.

Redington[81] has shown that the temperature dependence of the second virial coefficient B_{11} is not properly described by the model potentials. The second virial coefficient describes[84] deviations of the gas from the ideal gas law $pv = RT$ and is for rigid diatomic monomers given[85] as an integral of

$$b(T) = 1 - \exp[-V/(kT)], \tag{43}$$

with V being the intermonomer potential. V is 0 for well separated monomers and otherwise negative. Redington

argued that the model potentials (among those he considered were those of Poulsen *et al.*,[63] Klein *et al.*,[64] Jorgensen and Cournoyer,[66] and Jorgensen[67]) predict B_{11} to approach 0 to slow as a function of increasing temperature in the range 250–650 K compared with experiments on water and HCl. Especially HCl should resemble similarities with HF.

In order to get a qualitative understanding of this we will simply assume $b(T)$ to be nonzero only for $V < -\gamma kT$, where γ is some undefined constant in the range, say, 1–10. We will furthermore assume that B_{11} is proportional to the volume of that part of the integration region where $b(T) \neq 0$. Then for T being some 100 K ($\sim \gamma kT$ approximately some few tenths of an eV) the volume for which $b(T) \neq 0$ is much smaller for the first-principles results than for the model potential results (see Fig. 10). I.e., the much weaker dependence of the model potentials on the structural parameters is the reason for the discrepancy.

The geometries we have applied our first-principles method on are restricted to planar ones where the hydrogen atoms furthermore are considered placed on the line joining neighboring fluorine atoms. They are therefore not sufficiently general for determining new model potentials. However, we believe that improved model potentials should possess at least three important features. They should explicitly include variations in d_H such that (i) in the large d_F limit they approach the Morse potential fit (5) for the single monomer, and (ii) they are able to describe the changes in the optimal d_H value for fixed d_F in the range 4–6 a.u. Furthermore, as demonstrated here and in the work by Honda and Kitaura[83] they should explicitly include interactions between molecular orbitals. Finally, it is important that they are able to describe multimer effects beyond those of dimers.

VIII. CONCLUSION

In the present paper we have demonstrated how we from first-principles calculations on polymeric HF can obtain results that are important in understanding not only static ground state properties of this compound but also excited states and dynamical properties.

We have applied our first-principles local-density full-potential LMTO method for helical polymers to calculate the electronic ground state properties for a large number of fixed nuclear geometries for a single HF monomer (Sec. III) and a HF polymer (Sec. IV). The results agreed well with those obtained from experiments as well as from other theoretical methods. Especially, we find geometrical parameters of the polymer in better agreement with experiment than other theoretical methods find. However, the ionization potential was found to suffer from a general local-density failure to give correct ionization potentials for such systems.

In three subsequent sections we analyzed different parts of the geometry space in examining different properties of hydrogen fluoride.

In the first example (Sec. V) we considered solitonic excitations of the polymer. We found—within a model Hamiltonian—that the soliton-antisoliton pair with the lowest creation energy E_{sol} is a sharp kink-antikink pair with E_{sol} being some tenths of an eV. This energy is larger than that quoted by Yomosa[38] (< 0.21 eV) for a soliton in an α helix, but the difference is comparable with the difference in the hydrogen bond energy. On the other hand E_{sol} is comparable with that (0.42 eV) calculated by Su, Schrieffer, and Heeger[43,44] for polyacetylene. This we believe to be due to two opposite effects: the stronger nearest neighbor coupling for polyacetylene will increase E_{sol}, but the smaller dimerization energy will decrease it. The soliton induced states slightly outside the energy ranges of the bands. These states should appear as shoulders or extra peaks in photoabsorption spectra, and should thus offer a direct way of experimentally testing the validity of our model. We believe these shoulders or peaks to be general for solitons in hydrogen-bonded systems. Including approximate electrostatic interactions caused no changes in the general conclusion concerning the width and creation energy of a soliton but led to smaller shifts of the soliton induced states. We believe that this finding will not be changed by more proper treatments of the electrostatic fields caused by a soliton-antisoliton pair. Especially, the coupling between neighboring monomers will remain weak and the soliton and antisoliton will accordingly have almost vanishing widths. The model includes electronic interactions, which have not been considered earlier for solitons in hydrogen-bonded polymers. With modifications the model can be transferred to other polymers containing hydrogen bonds.

In a subsequent section (Sec. VI) we examined frequencies of frozen optical stretch phonons at the zone center. For a harmonic approximation we found frequencies in very good agreement with experiment. Because of the small mass of the hydrogen atoms we also considered a simple anharmonic double-well potential for a single isolated molecule. By solving the resulting Schrödinger equation numerically we found excitation frequencies in reasonable agreement with those just mentioned. Furthermore, we found excitation energies in the low-energy range, and finally we found excitation energies in an energy range where no absorption has been reported to our knowledge. Since the corresponding state is fairly delocalized coupling to neighboring sites could lead to shifts in the energies. Furthermore, we believe that it will have small Raman and infrared cross sections and therefore be difficult to observe.

In order to examine the coupling to the neighboring sites one could add kinetic energy terms of the nuclei to the model Hamiltonian used for examining the solitonic excitations and then consider the excitation energies of ring molecules as done in Sec. V. This could be a topic for a future paper.

Finally (Sec. VII), we compared our first-principles total energies with those predicted by simple model potentials used in examining the dynamics of the gas and liquid phases. Since these phases are known to consist partly of clusters of monomers it is important that the potentials can describe the "multimer" effects although they usually are derived from first-principles calculations on an isolated dimer. We found that none of the potentials could de-

scribe all the bond length relaxations when passing from the dimer to the polymer, that the energy differences between zigzag and linear chains were usually predicted to be too small, and that the energy surfaces in general were too flat. This could explain why the temperature dependence of the second virial coefficient is not reproduced correctly by the model potentials.

Note added. After submission of this manuscript we received[86] a revised version of the model potential by Redmon and Binkley.[72] With this we obtained the following results: In contrast to the other model potentials with electrostatic interactions between only two point charges per monomer this model correctly predicts the zigzag polymer (and for the dimer: the bent structure) to be the stable form. But as all the other model potentials of Fig. 10 it is not able to describe the molecular bond length relaxations upon forming the polymer from the monomers. Furthermore, the decrease in d_F when passing from the dimer to the polymer is substantially overestimated. Finally, as most of the model potentials of Fig. 10, this model also gives a too flat potential surface. Therefore, we do not believe this model potential to include all the effects that are important for understanding and describing multimers beyond dimers.

ACKNOWLEDGMENTS

Useful comments by Dr. Alfred Karpfen are gratefully acknowledged. Furthermore, the author wishes to thank Dr. Björn S. Nilsson for assistance in performing the numerical calculations. Many thanks are due to Dr. Alan Luther for a careful reading of the manuscript and to Dr. Alan Luther and Dr. Per Hedegård for useful comments.

[1]M. Atoji and W. N. Lipscomb, Acta Crystallogr. **7**, 173 (1954).
[2]S. P. Habuda and Y. V. Gagarinsky, Acta Crystallogr., Sect. B **27**, 1677 (1971).
[3]D. F. Smith, J. Chem. Phys. **28**, 1040 (1958).
[4]R. H. Maybury, S. Gordon, and J. J. Katz, J. Chem. Phys. **23**, 1277 (1955).
[5]J. W. Ring and P. A. Egelstaff, J. Chem. Phys. **51**, 762 (1969).
[6]M. Springborg and O. K. Andersen, J. Chem. Phys. **87**, 7125 (1987).
[7]M. Springborg, Phys. Rev. Lett. **59**, 2287 (1987).
[8]W. Kohn and L. J. Sham, Phys. Rev. **140**, A1133 (1965).
[9]U. von Barth and L. Hedin, J. Phys. C **5**, 1629 (1972).
[10]P.-O. Löwdin, Adv. Quantum Chem. **5**, 185 (1970).
[11]G. Di Lonardo and A. E. Douglas, Can. J. Phys. **51**, 434 (1973).
[12]K.-P. Huber and G. Herzberg, *Constants of Diatomic Molecules* (Van Nostrand Reinhold, New York, 1979).
[13]D. R. Yarkony, S. V. O'Neil, H. F. Schaefer III, C. P. Baskin, and C. F. Bender, J. Chem. Phys. **60**, 855 (1974).
[14]M. Karplus and R. N. Porter, *Atoms and Molecules: An Introduction for Students of Physical Chemistry* (Benjamin, New York, 1970).
[15]H.-J. Werner and P. Rosmus, J. Chem. Phys. **73**, 2319 (1980).
[16]S. B. Trickey, Phys. Rev. Lett. **56**, 881 (1986).
[17]G. Bieri, A. Schmelzer, L. Asbrink, and M. Jonsson, Chem. Phys. **49**, 213 (1980).
[18]R. J. Bartlett, Annu. Rev. Phys. Chem. **32**, 359 (1981).
[19]C.-M. Liegener and J. Ladik, Phys. Rev. B **35**, 6403 (1987).
[20]M. W. Johnson, E. Sándor, and E. Arzi, Acta Crystallogr., Sect. B **31**, 1998 (1975).
[21]A. Karpfen, J. Ladik, P. Russegger, P. Schuster, and S. Suhai, Theor. Chim. Acta (Berlin) **34**, 115 (1974).
[22]J. Bacon and D. P. Santry, J. Chem. Phys. **56**, 2011 (1972).
[23]R. W. Crowe and D. P. Santry, Chem. Phys. Lett. **45**, 44 (1977).
[24]A. Zunger, J. Chem. Phys. **63**, 1713 (1975).
[25]R. Lochmann, Int. J. Quantum Chem. **12**, 851 (1977).
[26]M. Kertész, J. Koller, and A. Ažman, Chem. Phys. Lett. **36**, 576 (1975).
[27]A. Karpfen, Chem. Phys. **47**, 401 (1980).
[28]A. Karpfen, A. Beyer, and P. Schuster, Int. J. Quantum Chem. **19**, 1113 (1981).
[29]A. Beyer and A. Karpfen, Chem. Phys. **64**, 343 (1982).
[30]Y. J. I'Haya, S. Narita, Y. Fujita, and H. Ujino, Int. J. Quantum Chem. Symp. **18**, 153 (1984).
[31]P. Otto and E. O. Steinborn, Solid State Commun. **58**, 281 (1986).
[32]R. W. Jansen, R. Bertoncini, D. A. Pinnick, A. I. Katz, R. C. Hanson, O. F. Sankey, and M. O'Keeffe, Phys. Rev. B **35**, 9830 (1987).
[33]L. Pietronero and N. O. Lipari, J. Chem. Phys. **62**, 1796 (1975).
[34]A. S. Davydov and N. I. Kislukha, Phys. Status Solidi B **59**, 465 (1973).
[35]A. S. Davydov and N. I. Kislukha, Zh. Eksp. Teor. Fiz. **71**, 2090 (1976) [Sov. Phys.—JETP **44**, 571 (1976)].
[36]A. S. Davydov, Phys. Scr. **20**, 387 (1979).
[37]S. Takeno, Prog. Theor. Phys. **73**, 853 (1985).
[38]S. Yomosa, Phys. Rev. A **32**, 1752 (1985).
[39]H. Bolterauer and R. D. Henkel, Phys. Scr. **T13**, 314 (1986).
[40]E. W. Laedke, K. H. Spatschek, M. Wilkens, Jr., and A. V. Zolotariuk, Phys. Rev. A **32**, 1161 (1985).
[41]C. K. Chiang, C. R. Fincher, Jr., Y. W. Park, A. J. Heeger, H. Shirakawa, E. J. Louis, S. C. Gau, and A. G. MacDiarmid, Phys. Rev. Lett. **39**, 1098 (1977).
[42]H. W. Streitwolf, Phys. Status Solidi B **127**, 11 (1985).
[43]W. P. Su, J. R. Schrieffer, and A. J. Heeger, Phys. Rev. Lett. **42**, 1698 (1979).
[44]W. P. Su, J. R. Schrieffer, and A. J. Heeger, Phys. Rev. B **22**, 2099 (1980); **28**, 1138(E) (1983).
[45]J. F. Nagle, M. Mille, H. J. Morowitz, J. Chem. Phys. **72**, 3959 (1980).
[46]M. Springborg, H. Kiess, and P. Hedegård (unpublished).
[47]L. Pietronero, Chem. Phys. **6**, 455 (1974).
[48]L. Pietronero, Solid State Commun. **17**, 961 (1975).
[49]A. Karpfen and P. Schuster, Chem. Phys. Lett. **44**, 459 (1976).
[50]P. W. Higgs, Proc. R. Soc. London, Ser. A **220**, 472 (1953).
[51]L. Piseri and G. Zerbi, J. Chem. Phys. **48**, 3561 (1968).
[52]K. Kunc and R. M. Martin, in *Ab Initio Calculation of Phonon Spectra*, edited by J. T. Devreese, V. E. van Doren, and P. E. van Camp (Plenum, New York, 1983).
[53]J. M. Lisy, A. Tramer, M. F. Vernon, and Y. T. Lee, J. Chem. Phys. **75**, 4733 (1981).
[54]J. S. Kittelberger and D. F. Hornig, J. Chem. Phys. **46**, 3099

(1967).
[55]A. Anderson, B. H. Torrie, and W. S. Tse, Chem. Phys. Lett. **70**, 300 (1980).
[56]B. Desbat and P. V. Huong, J. Chem. Phys. **78**, 6377 (1983).
[57]R. Tubino and G. Zerbi, J. Chem. Phys. **51**, 4509 (1969).
[58]W.-S. Tse and C.-N. Chang, Phys. Status Solidi B **119**, 349 (1983).
[59]J. F. Higgs, W. Y. Zeng, and A. Anderson, Phys. Status Solidi B **133**, 475 (1986).
[60]A. Axmann, W. Biem, P. Borsch, F. Hossfeld, and H. Stiller, Discuss. Faraday Soc. **48**, 69 (1969).
[61]P. Janoschek, in *The Hydrogen Bond,* edited by P. Schuster, G. Zundel, and C. Sandorfy (North-Holland, Amsterdam, 1976).
[62]J. Brickmann and H. Zimmermann, J. Chem. Phys. **50**, 1608 (1969).
[63]L. L. Poulsen, G. D. Billing, and J. I. Steinfeld, J. Chem. Phys. **68**, 5121 (1978).
[64]M. L. Klein, I. R. McDonald, and S. F. O'Shea, J. Chem. Phys. **69**, 63 (1978).
[65]I. R. McDonald and M. L. Klein, Discuss. Faraday Soc. **66**, 48 (1978).
[66]W. L. Jorgensen and M. E. Cournoyer, J. Am. Chem. Soc. **100**, 4942 (1978).
[67]W. L. Jorgensen, J. Am. Chem. Soc. **100**, 7824 (1978).
[68]W. L. Jorgensen, J. Chem. Phys. **70**, 5888 (1979).
[69]M. L. Klein and I. R. McDonald, J. Chem. Phys. **71**, 298 (1979).
[70]M. E. Cournoyer and W. L. Jorgensen, Mol. Phys. **51**, 119 (1984).
[71]S. Murad, K. A. Mansour, and J. G. Powles, Chem. Phys. Lett. **131**, 98 (1986).
[72]M. J. Redmon and J. S. Binkley, J. Chem. Phys. **87**, 969 (1987).
[73]M. A. Spackman, J. Chem. Phys. **85**, 6587 (1986).
[74]D. W. Schwenke, D. G. Truhlar, and M. E. Coltrin, J. Chem. Phys. **87**, 983 (1987).
[75]M. A. Spackman, J. Chem. Phys. **85**, 6579 (1986).
[76]P. E. Cade and W. Huo, At. Data Nucl. Data Tables **12**, 415 (1973).
[77]D. W. Michael, C. E. Dykstra, and J. M. Lisy, J. Chem. Phys. **81**, 5998 (1984).
[78]P. N. Swepston, S. Colby, H. L. Sellers, and L. Schäfer, Chem. Phys. Lett. **72**, 364 (1980).
[79]S.-Y. Liu, D. W. Michael, C. E. Dykstra, and J. M. Lisy, J. Chem. Phys. **84**, 5032 (1986).
[80]J. H. Clark, J. Emsley, D. J. Jones, and R. E. Overill, J. Chem. Soc. Dalton Trans. **1981**, 1219 (1981).
[81]R. L. Redington, J. Chem. Phys. **75**, 4417 (1981).
[82]T. R. Dyke, B. J. Howard, and W. Klemperer, J. Chem. Phys. **56**, 2442 (1972).
[83]K. Honda and K. Kitaura, Chem. Phys. Lett. **140**, 53 (1987).
[84]F. J. Wilkins, Proc. R. Soc. London, Ser. A **164**, 496 (1938).
[85]J. O. Hirschfelder, C. F. Curtiss, and R. B. Bird, *Molecular Theory of Gases and Liquids* (Wiley, New York, 1954).
[86]M. J. Redmon (private communication).